



# The Miocene record of the Betic Cordillera uplift in Los Guájares valley (Granada province, S Spain)

Tomás Alberjón-Peñas<sup>1</sup>  · Juan C. Braga<sup>1</sup> · Julio Aguirre<sup>1</sup> · Paola Flórez<sup>1</sup>

Received: 28 October 2022 / Accepted: 12 May 2023 / Published online: 30 May 2023  
© The Author(s) 2023

## Abstract

The Los Guájares valley is located about 35 km south of Granada in the Internal Zones of the Betic Cordillera. The Miocene deposits in this area consist of six sedimentary units separated by unconformities, which are exposed in small and laterally discontinuous outcrops overlying metamorphic rocks of the Alpujárride Complex. The lowest unit comprises upper Serravalian marls with planktonic foraminifera filling neptunian dykes and covering Triassic dolomitic marbles of the Alpujárride Complex. These marls reflect deep marine deposition on the Betic basement under a local extensional regime. Uplift of the region led to emergence and deposition of continental red alluvial-fan conglomerates and foothill breccias. The overlying unit, a shoreline conglomerate with small oyster banks, indicates relative sea-level rise. Shallow-marine conditions continued during the deposition of the following unit, early Tortonian in age, which consists of calcareous sandstones with hermatypic corals. Small patch reefs developed in the overlying unit composed of sandy limestones with corals (*Porites*, *Tarbellastrea*, *Thegioastraea*) and oysters, and sandy limestones with coralline algae in the most distal areas. The coral reefs in Los Guájares and some coral heads in Albuñuelas, a near locality, are the only record of early Tortonian coral buildups in the Mediterranean. The last marine unit comprises lower Tortonian conglomerates, sandstones and siltstones accumulated in the front of a small delta. Oyster banks and concentrations of *Turritelines* suggest high nutrient levels in the delta-front paleoenvironments. The Los Guájares valley area emerged afterwards, following the onset of a compressional geodynamic regime in the central Betic Cordillera and since the early Tortonian only small bodies of foothill and alluvial-fan deposits formed in a predominantly erosional context.

**Keywords** Early Tortonian · Coral reefs · Western Mediterranean · Biostratigraphy · Betic Cordillera

## El registro del levantamiento de la Cordillera Bética durante el Mioceno en el valle de Los Guájares (provincia de Granada, sur de España)

### Resumen

El valle de Los Guájares se encuentra a unos 35 km al sur de Granada en las Zonas Internas de la Cordillera Bética. Los depósitos del Mioceno en esta área consisten en seis unidades sedimentarias, separadas por discordancias, que están expuestas en pequeños afloramientos lateralmente discontinuos sobre rocas metamórficas del Complejo Alpujárride. La unidad inferior comprende margas del Serravalliense superior con foraminíferos planctónicos que rellenan diques neptúnicos y cubren dolomías triásicas del Complejo Alpujárride. Estas margas son sedimentos marinos profundos acumulados sobre el basamento bético bajo un régimen extensional local. El levantamiento de la región condujo a la emersión y al depósito de conglomerados rojos continentales, formados en abanicos aluviales, y de brechas de pie de monte. La unidad suprayacente, un conglomerado costero con pequeños bancos de ostras, indica un aumento relativo del nivel del mar que invadió la zona.

---

✉ Tomás Alberjón-Peñas  
tomasalberjon@ugr.es

<sup>1</sup> Departamento de Estratigrafía y Paleontología, Facultad de Ciencias, Universidad de Granada, Campus Fuentenueva, 18002 Granada, Spain

Las condiciones marinas poco profundas continuaron durante el depósito de la siguiente unidad, de edad Tortoniense inferior, que consiste en areniscas calcáreas con corales hermatípicos. Por encima, la siguiente unidad está compuesta por calizas arenosas con pequeños parches arrecifales de coral (*Porites*, *Tarbellastraea*, *Thegioastraea*) y ostras, y por calizas arenosas con algas coralinas en las áreas más distales. Los parches arrecifales de coral en Los Guájares y algunos pequeños domos de coral en Albuñuelas, una localidad cercana, son el único registro de bioconstrucciones coralinas del Tortoniense inferior en el Mediterráneo. La última unidad marina comprende conglomerados, areniscas y limos del Tortoniense inferior acumulados en el frente de un pequeño delta. Los bancos de ostras y las concentraciones de turrítelinos sugieren altos niveles de nutrientes en los paleoambientes del frente del delta. El área del valle de Los Guájares emergió posteriormente, siguiendo la instalación de un régimen geodinámico compresivo en la Cordillera Bética central, y desde el Tortoniense inferior sólo se formaron pequeños cuerpos de depósitos de pie de monte y abanicos aluviales en un contexto predominantemente erosivo.

**Palabras Clave** Tortoniense inferior · Arrecifes de coral · Mediterráneo occidental · Bioestratigrafía · Cordillera Bética

## 1 Introduction

The Miocene sedimentary rocks that appear in small outcrops in the Internal Zones of the Betic Cordillera have been poorly studied, and the knowledge on their origin and relationships with adjacent larger basins, such as the Granada Basin is limited. This is the case of the Miocene deposits in the Los Guájares valley (Granada), which have only been reported in studies on the regional geology of the area. These works comprise the sheet 1041 (Dúrcal) of the MAGNA geological map from the late 1970s (Avidad et al., 1978), and a paper by Estévez et al. (1985), where the authors include a lithological map and a brief description of the stratigraphy of the Neogene to Quaternary cover on the metamorphic basement. The latter work points out the complex stratigraphy of the Miocene materials, which are faulted and folded and crop out in small, dispersed exposures. The described lithological succession reflects drastic changes in the depositional environments, which record the uplift history of this part of the Betic mountains in the Middle and early Late Miocene. Lower and Middle Miocene deposits in the Internal Zones of the Betic Cordillera generally occur in highly tectonized, scattered outcrops at the base of the sedimentary fillings of the Neogene intermontane basins (González-Donoso, 1978; Hodgson, 2002; Rodríguez-Fernández, 1982; Rondeel, 1965). Limited lateral and vertical exposures, unconformities and facies heterogeneity make difficult correlation and paleoenvironmental interpretation of the successive sedimentary units even if the age of some of them was constrained with planktonic foraminifer and nannoplankton biostratigraphy, strontium isotope stratigraphy and fission track thermochronology (González-Donoso, 1978; Hodgson, 2002; Johnson et al., 1998; Rodríguez-Fernández, 1982; Rondeel, 1965). This prevents an accurate reconstruction of the paleogeographical evolution of the region in a key period of exhumation and emergence of the cordillera.

The scarcity of data on coral reefs of early Tortonian age all over the Mediterranean region (Perrin & Bosellini, 2012) made worth a detailed study of the structure and composition of the coral reefs in Los Guájares valley reported by Estévez et al. (1985).

The primary aim of this work is to analyze the sedimentological features and fossil content of the successive lithostratigraphic units that can be distinguished in the Miocene rocks in the Los Guájares valley. Specific purposes are: (a) to establish a precise age of the largest possible number of units and correlate them with materials deposited in the Granada Basin, the nearest basin with a relatively well-developed and well-known Miocene sedimentary record; (b) to interpret the depositional paleoenvironments of each unit, as well as the sedimentary evolution of the area; and (c) to characterize the coral reefs in the area in the context of coral-reef decline in the Mediterranean region.

## 2 Geographical and geological context

The study area is located in the Los Guájares valley, an area of approximately 90 km<sup>2</sup>, about 35 km south of Granada, in southern Spain (Fig. 1). The Miocene deposits crop out between the villages of Guájar-Faragüit and Guájar-Alto, and cover about 5 km<sup>2</sup> (Fig. 2). The area belongs to the Internal Zones of the Betic Cordillera, the westernmost segment of the European Alpine belt. The cordillera can be divided into three main domains: (1) the External Zones that represent the Mesozoic to Middle Miocene southern continental margin of the Iberian Massif (García-Hernández et al., 1980; Vera, 1988); (2) the Campo de Gibraltar or Flysch Units that comprise a series of allochthonous, Cretaceous to Middle Miocene units (e.g., Sanz de Galdeano & Vera, 1992); and (3) the Internal Zones, mainly made

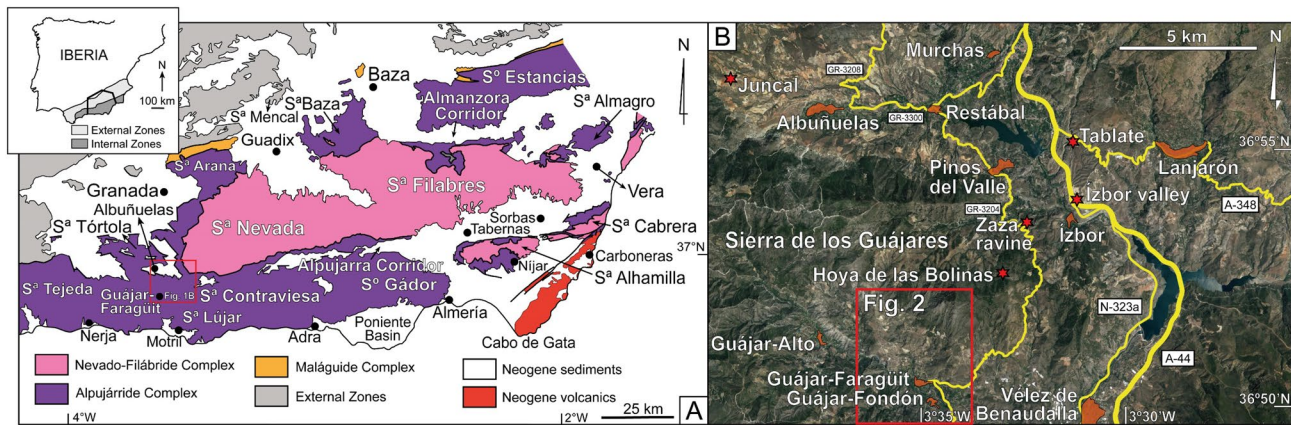


**Fig. 1** **A** Simplified geological map of the Betic Cordillera and situation of the study area (Los Guájares valley, red square) in the Internal Zones. **B** Access roads to the Los Guájares valley and adjacent villages (yellow). Localities mentioned in the text marked with red stars

up of metamorphic rocks (Fallot, 1948). The latter domain includes three stacked tectonic complexes, which in ascending order are: the Nevado-Filábride Complex (Paleozoic or older) (Gómez-Pugnaire et al., 2000, 2004), the Alpujarride Complex (Paleozoic to Mesozoic metasediments) (Delgado et al., 1981), and the Maláguide Complex, with a non-metamorphic Mesozoic to Cenozoic cover overlying a pre-Permian basement (Lonergan, 1993; Martín-Martín, 1996). The Miocene sedimentary rocks of the Los Guájares valley overlie rocks of the Alpujarride Complex, concentrating in grabens delimited by normal faults (Fig. 2). In the Los Guájares area, the Alpujarride Complex includes two units, the so-called Los Guájares and La Herradura nappes. These units, Paleozoic to Triassic in age, basically consist of graphitic schists, quartzites, calcschists and calcitic-dolomitic marbles (Avidad et al., 1978) (Fig. 2).

### 3 Methods

Twelve stratigraphic sections were logged in dispersed exposures along roads and in ravines in the Miocene outcrops in Los Guájares valley (Figs. 3, 4). The lithological, sedimentological and paleontological characteristics, geometry and thickness variations of the sedimentary bodies, and significant stratigraphic surfaces were observed at the outcrops and the main distinguished units were mapped at 1:20,000 scale (Fig. 2). Macrofossils were collected for identification in the laboratory. Twenty-six thin sections were prepared from rock samples for petrographic analysis and identification of biogenic components in the laboratory. Calcimetry was performed on four samples to determine their calcium carbonate content. To extract foraminifera for biostratigraphic dating and paleoenvironmental interpretation, 16 samples of fine-grained sediments were washed using sieves of 0.25,

0.125 and 0.065 mm and then dried in an oven at 40°C. The residue in the 0.125 mm fraction was the one examined. The extracted foraminifera were examined under an optical microscope Leica MZ12 and under a SEM Quanta 650 FEG (Thermofisher-FEI).

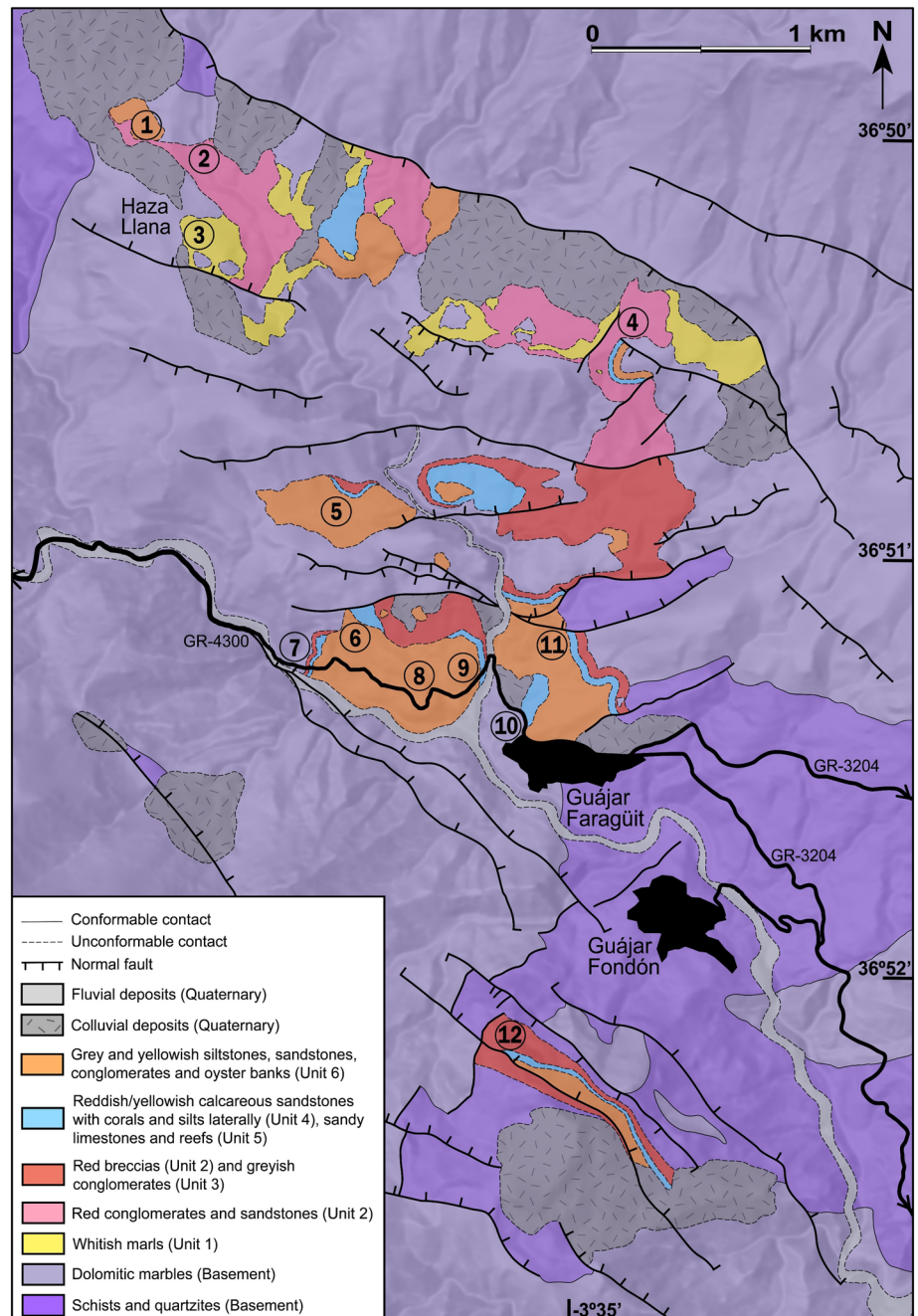
## 4 Lithostratigraphic units and paleontological content

In the twelve stratigraphic sections logged (Figs. 2, 3, 4), six units were identified based on lithology, fossil content and boundary surfaces (Fig. 5). From the lowest to the youngest these are:

### 4.1 Unit 1

This is the basal unit, directly overlying the dolomitic marbles of the Alpujarride Complex. It is laterally very discontinuous, appearing on the basement in numerous outcrops in the Haza Llana area and disappearing completely towards the south (Fig. 2). In Sect. 2 (Fig. 3), the unit is made up of whitish marls with heterometric angular clasts of the basement, up to 30 cm in size. The marls occur as a lens-shaped body approximately 2 m wide and 1 m thick, and do not contain fossils. In Sect. 3, about 450 m south of Sect. 2 (Figs. 2, 3), well-lithified whitish marls fill in neptunian dikes in the basement marbles (Fig. 6A) and pass vertically to a more continuous bed of friable marls about 1 m thick. The fillings of the neptunian dykes are wackestones with angular marble fragments and abundant planktonic foraminifera (Fig. 6B), in contrast with the overlying marls, which contain altered specimens. The identified planktonic foraminifera are *Globigerina*

**Fig. 2** Geological map of the study area. The location of logged sections (Figs. 3, 4) is indicated by numbers 1 to 12. Units 2 and 3, and 4 and 5, respectively, are mapped together due to their small extension



spp., *Paragloborotalia continuosa* (Blow), *Paragloborotalia mayeri* (Cushman & Ellisor), *Paragloborotalia siakensis* (LeRoy), *Orbulina suturalis* Brönnimann, and *Globigerinita glutinata* (Egger). Benthic foraminifera are dominated by *Cibicides*, *Cibicoides*, *Pullenia*, *Melonis*, and *Uvigerina*.

#### 4.2 Unit 2

In the Haza Llana area (Sects. 1, 2, 3 and 4, Figs. 2, 3), this unit appears as a horizontally bedded, reddish

conglomerate overlying an erosion surface. The conglomerate, up to 4 m thick, is highly heterometric, matrix-supported and without fossils. The clasts are mostly subrounded cobbles of dolomitic marbles. Locally, alternations of reddish and grey conglomerates, and sandstones can be observed. To the south, the unit abruptly changes along a direct fault plane (Figs. 2, 5) to a strongly lithified, clast-supported breccia, with a red terrigenous matrix (Fig. 6C). This breccia is structureless, up to 15 m in thickness, highly heterometric, with pebbles to boulders up to 100 cm in size and without fossils. The clasts are

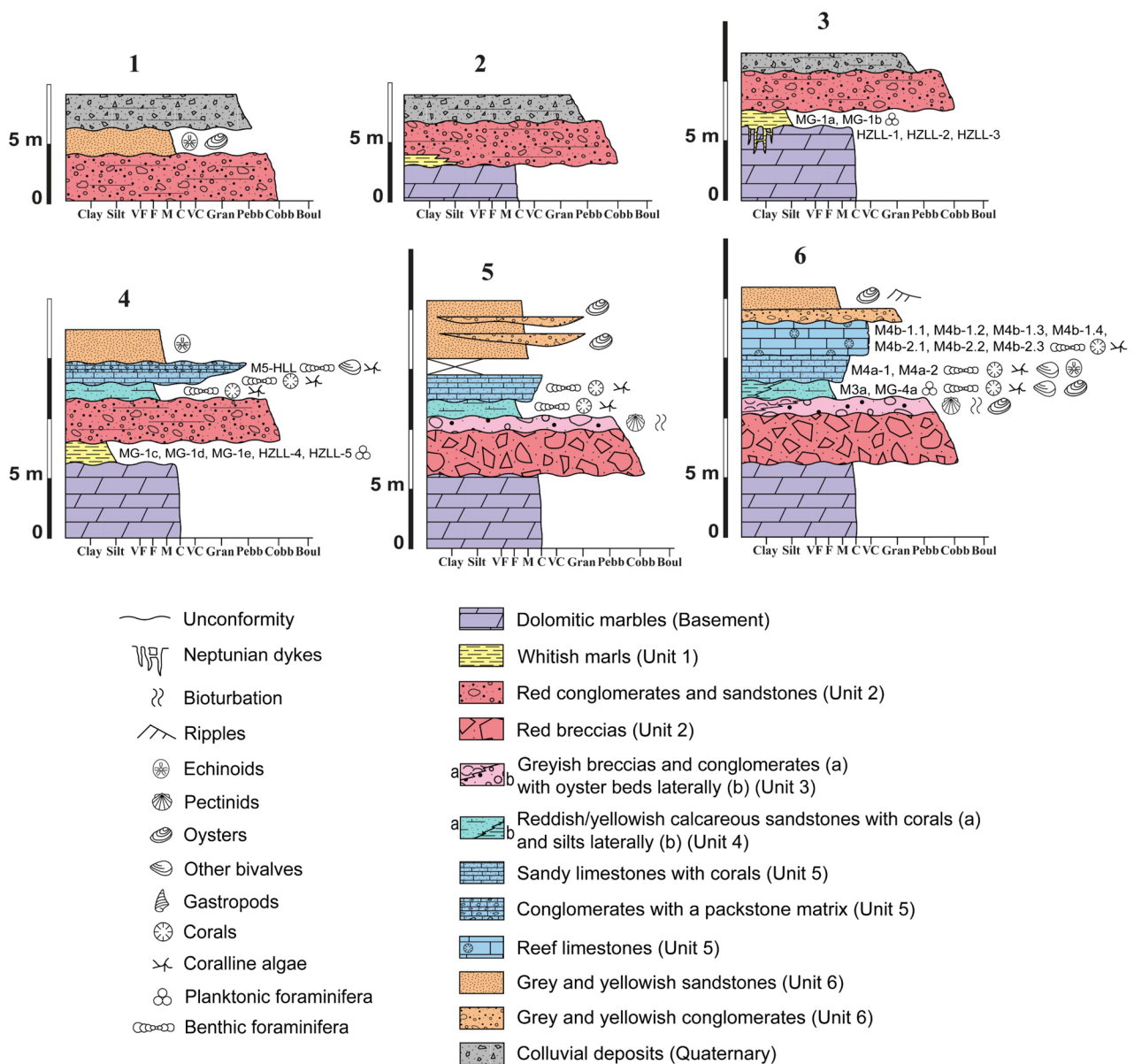


**Fig. 3** Stratigraphic Sects. 1–6. Location indicated in Fig. 2. Position of samples marked by labels; MG- labels indicate washed fine-grained sediments

carbonate fragments from the basement (dolomitic marbles and calcschists), except southeast of Sect. 12 (Figs. 2, 4), where the clast-supported breccia contains numerous angular clasts made up almost exclusively of schists because it lies directly on top of graphite schists. Poorly developed paleosols and rough horizontal stratification can be observed. Larger blocks (20–40 cm) appear concentrated in some beds. The unit overlies a karst surface carved on the basement in Sect. 9 (Figs. 2, 4).

### 4.3 Unit 3

It overlies an erosion surface on Unit 2 and consists of a thin, up to 1.5 m thick, laterally discontinuous matrix-supported breccia changing upwards to conglomerate with a greyish matrix. The breccia is structureless and heterometric. Clasts are carbonate and quartzite fragments from the Alpujarride basement. The predominantly angular clasts at the base change to more rounded at the top. The clast size varies from pebble to cobble (up to 20 cm). Carbonate clasts bored by bivalves (*Gastrochaenolites* isp.) and small specimens of *Chlamys* sp. can be observed. Small oysters

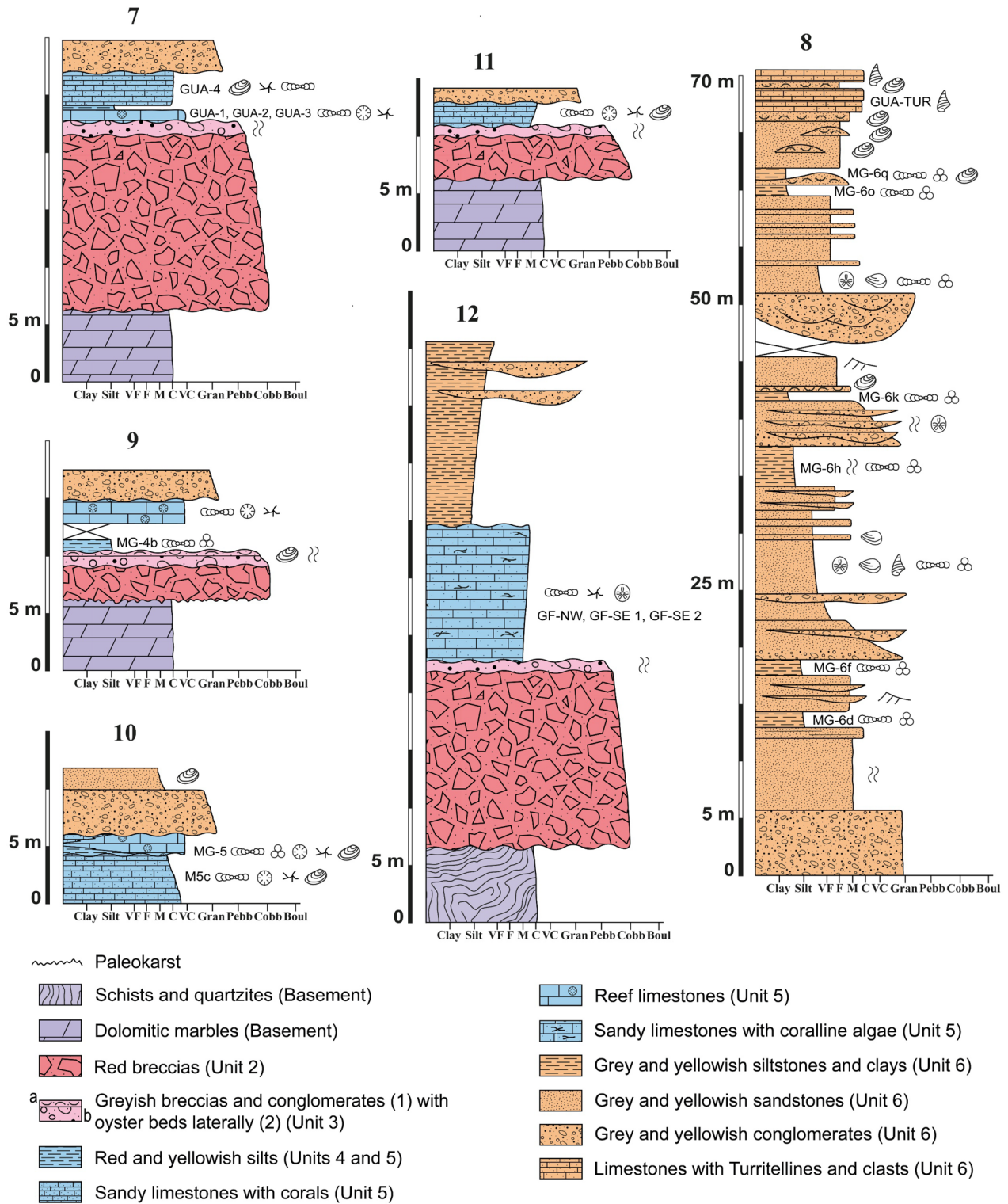


**Fig. 4** Stratigraphic Sects. 7–12. Location indicated in Fig. 2. Position of samples marked by labels; MG- labels indicate washed fine-grained sediments. Fossil and surface symbols in Fig. 3

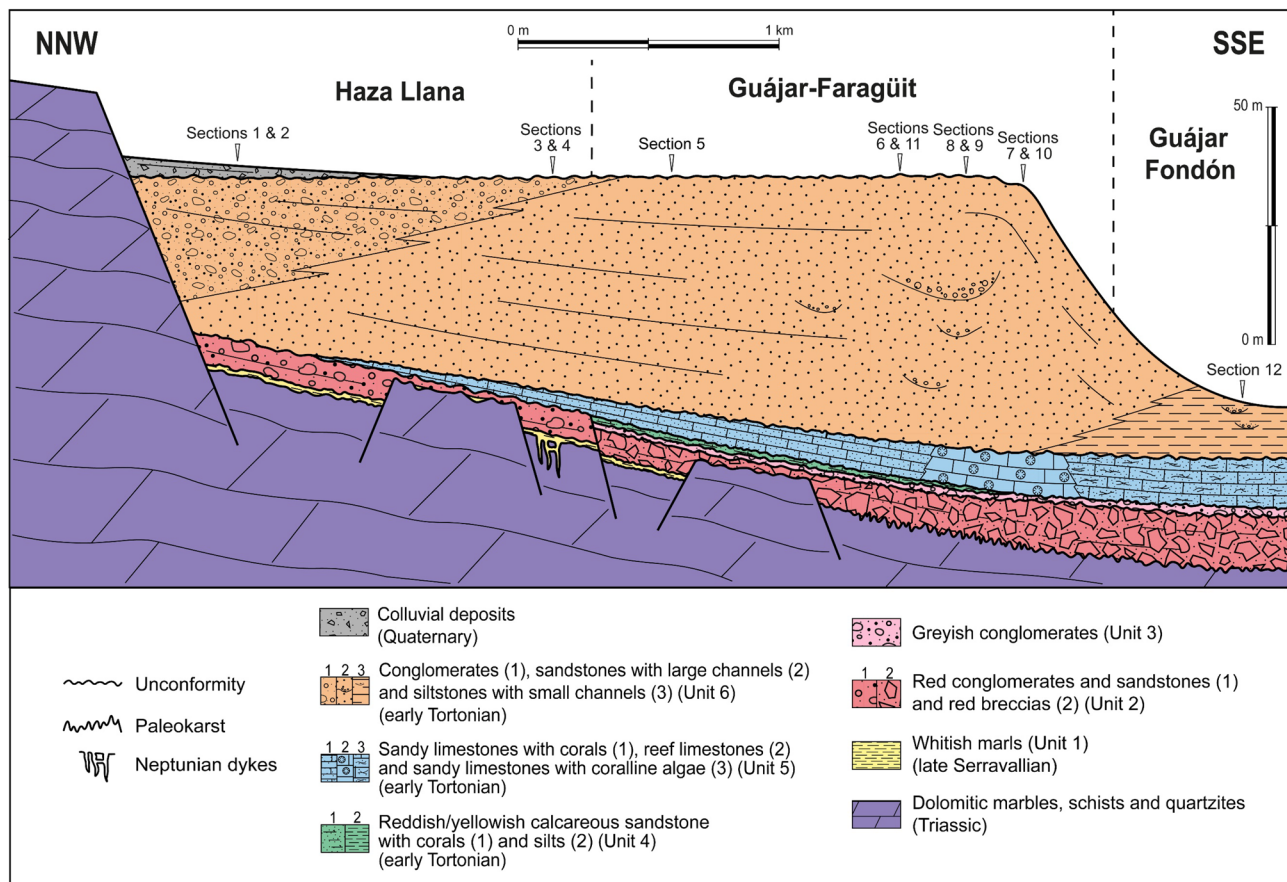


**Fig. 5** Idealized stratigraphic scheme of the Miocene rocks in the Los Guájares valley

occur in life position colonizing the clasts at the top of the unit. Patches of oysters, up to 4 m wide and 80–90 cm thick, appear directly above the conglomerates in Sects. 6 and 9 (Figs. 2, 3, 4). These patches are built by *Ostrea edulis* Linné and *Magallana gryphoides* (Schlotheim). The oysters are fragmented at the base whilst some valves are almost complete, up to 20 cm in size, towards the top.

#### 4.4 Unit 4

This is a mixed terrigenous-carbonate unit, which is characterized by complex lateral facies changes. In Sects. 4, 5, 6 and 11 (Figs. 2, 3, 4), the unit is up to 2 m thick, and thins and disappears laterally. In Sect. 6 (Figs. 2, 3), this unit overlies an erosion surface, adapting to a series of paleosteps carved on the underlying Unit 3. Unit 4 comprises a granule to pebble conglomerate at the base that passes upwards to reddish or yellowish fine-grained calcareous sandstone (21% of  $\text{CaCO}_3$  content), with dispersed fragments of crustose coralline algae, such as *Lithophyllum* sp. and *Neogoniolithon* sp., and fragments of the coral *Porites* sp. The sandstone laterally includes larger fragments of branching colonies of

*Porites* sp. that give a nodular aspect to the rock. In Sect. 6 (Figs. 2, 3), isolated head-shaped colonies of *Tarbellastraea* sp., approximately 30–40 cm wide and 30 cm thick, can be observed in life position attached on top of the paleosteps, although they are also found embedded within the sandy matrix. The calcareous sandstone is rich in internal molds of bivalves of the order Lucinida, such as *Lucina gracilis* (Nyst), and some unidentified specimens of the order Nuculanida. There are also shells of calcitic bivalves, such as *Pecten* sp., *Chlamys* sp. and *Spondylus* sp., and some small specimens of *O. edulis*.

In Sects. 6 and 9 (Figs. 2, 3, 4), the calcareous sandstone passes laterally southwards to siltstones (Fig. 5), which contain very scarce foraminifera (they represent less than 1% of the residue). Among planktonic foraminifera, *Catapsydrax unicavus* Bolli, Loeblich & Tappan, *Globigerina bulloides* (d'Orbigny), *Paragloborotalia continua* (Blow), *Globigerinita glutinata* (Egger), and *Orbulina suturalis* Brönnimann have been identified. Benthic foraminifera are extremely rare, mostly represented by a few specimens of *Cibicides*, *Elphidium*, and *Nonion*. This facies appears in several outcrops with limited lateral continuity.

**Fig. 6** **A** Field photograph showing well-lithified whitish marls (Unit 1) filling in neptunian dykes in the basement dolomitic marbles at Sect. 3. Coin = 2.3 cm. **B** Thin-section micrograph of planktonic-foraminifer wackestone-packstone with basement clasts in filling in dykes in A (sample HZLL-2). **C** Clast-supported breccia with a red matrix (Unit 2 at Sect. 6). Hammer length = 33 cm



#### 4.5 Unit 5

In Sects. 5, 6 and 11, it consists of sandy limestones (52% of carbonate content) overlying an erosion surface cutting Units 3 and 4 (Figs. 2, 3, 4). They are terrigenous wackestones/packstones with *Porites* and *Tarbellastraea* colonies. Abundant branching and nodular colonies of *Porites* sp. intergrown with and encrusted by coralline algae (*Lithophyllum* sp., *Neogoniolithon* sp., and *Spongites* sp.) give a nodular aspect to the rock. The sandy reddish matrix is generally fine-grained, although locally it passes to patches with greenish colors richer in terrigenous grains of medium to coarse size. Together with the branching colonies of *Porites* sp., there are isolated heads of *Tarbellastraea* sp. in life position. *Porites* is more abundant than *Tarbellastraea*. Well-preserved isolated specimens of *O. edulis* and whole clypeasteroid echinoids can also be found. At some sites, such as Sect. 6 (Figs. 2, 3), small coral patches overlie the sandy nodular limestones, forming bodies that range between 1 and 1.5 m in thickness and

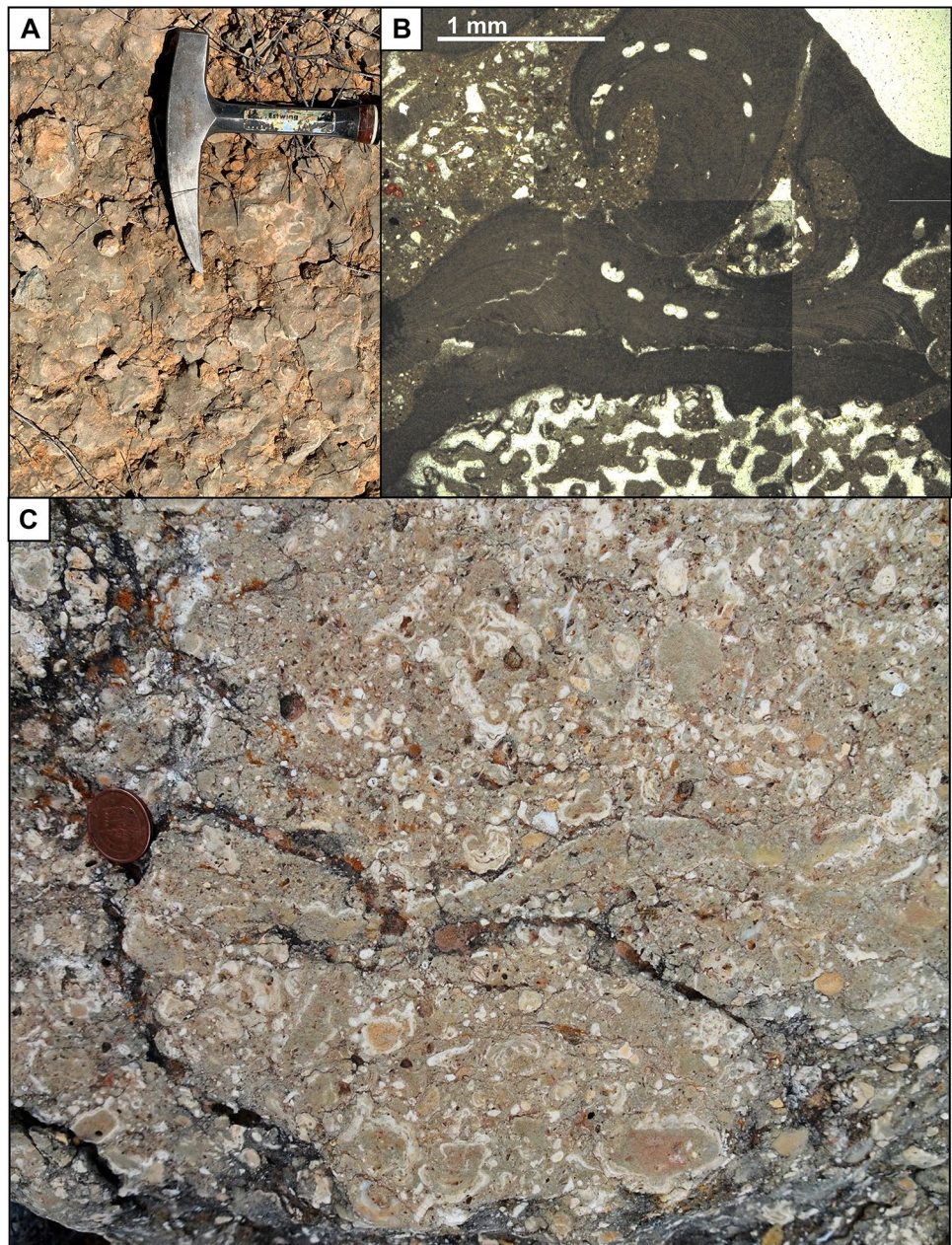
15–20 m in width. They consist of head-shaped colonies of *Porites* sp. and *Tarbellastraea* sp., and coralline algae, which appear both encrusting corals and as small nodules dispersed in the wackestone matrix (Fig. 7A, B). *Lithophyllum* gr. *racemus*, *Lithophyllum* gr. *nitorum*, *Neogoniolithon* sp., and *Spongites* sp. were identified in the patches.

At the base of Sect. 7 (Figs. 2, 4), the unit consists of a bioherm structure, formed by colonies of *Tarbellastraea abditaxis* Chevalier in life position, locally encrusted by coralline algae (*Lithophyllum* sp., *Lithophyllum* gr. *nitorum*, *Neogoniolithon* sp., and *Spongites* sp.). These coralline algae also appear as nodules in the wackestone matrix. This bioherm is covered by a thin bed of yellowish siltstone, 30–40 cm thick, which in turn is overlain by a 2 m thick package of packstone rich in *O. edulis*.

In Sect. 10 (Figs. 2, 4, 8A), fine- to coarse-grained calcareous sandstones (30% to 38% of carbonate content) occur at the base of the unit. They are dark due to fragments of dolostone and schists from the basement, and contain larger benthic foraminifera, such as *Borelis* sp., gastropods and



**Fig. 7** **A** Reef limestone with small branching *Porites* colonies (Unit 5 at Sect. 6). Note coralline algae encrusting corals. Hammer head = 18 cm. **B** Thin-section micrograph of *Lithophyllum* gr. *racemus* encrusting *Porites* sp. (sample GUA-2). **C** Sandy limestones with coralline algae forming rhodoliths, some of them with coral nuclei (Unit 5 at Sect. 12). Coin = 2.1 cm



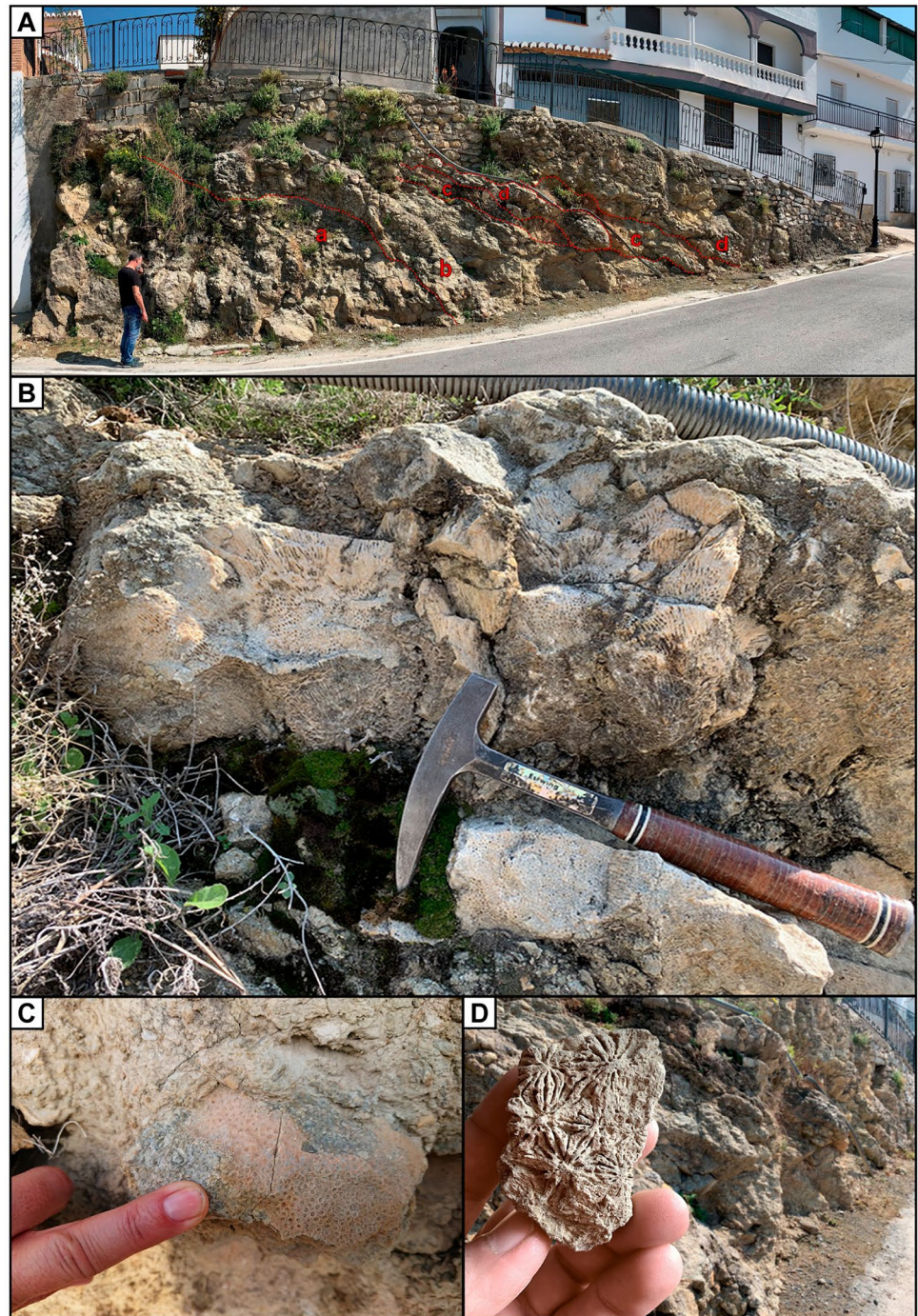
bivalves. The calcareous sandstones change upwards to sandy limestones with branching *Porites* colonies similar to those in Sects. 5, 6 and 11 (Figs. 2, 3, 4). They are overlain by reddish silts interspersed with two patch reefs formed by head-shaped colonies of *T. abditaxis*, up to 50 cm wide and 45 cm thick (Fig. 8B, C), some laminar colonies of *Tarbelastrea* sp., head-shaped *Porites* colonies and *Thegioastrea* sp. (Fig. 8D). A thin lens of sandy limestone rich in *O. edulis* appears among the coral patches. Isolated specimens of *Hytissa hyotis* (Linné) occur attached to the coral colonies. Planktonic (*Globigerinoides* spp.) and benthic foraminifera (*Praeglobobulimina pupoides* (d'Orbigny), *Anomalinoidea*

*flinti* (Cushman), *Cancris oblongus* (Williamson), and *Melonis soldanii* (d'Orbigny)) have been recognized in the reddish silts.

In outcrops in the Haza Llana area (Fig. 2), this unit consists of nodular sandy limestones, up to 2 m thick, which at Sect. 4 (Figs. 2, 3) are capped by a conglomerate of sub-angular pebbles of dolomitic marble and quartzite, with a packstone matrix with larger benthic foraminifera (*Nummulitidae*), bivalves and coralline algae as the main bioclastic components.

South of Guájar-Fondón, in Sect. 12 (Figs. 2, 4), the unit consists of sandy limestones, up to 20 m thick, with abundant

**Fig. 8** **A** Unit 5 at Sect. 10. **a** Fine-to coarse-grained calcareous sandstones. **b** Sandy limestones with branching *Porites* colonies. **c** Reddish silts. **d** Patch reefs formed by head-shaped colonies of *Tarbellastraea abditaxis*, laminar colonies of *Tarbellastraea* sp., head-shaped *Porites* colonies and *Thegioastraea* sp. Man is 1.70 m tall. **B** Head-shaped *T. abditaxis* colony (Unit 5 at Sect. 10). Hammer length = 33 cm. **C** Detail of *T. abditaxis* (Unit 5 at Sect. 10). Finger width = 1.6 cm. **D** Fragment of *Thegioastraea* sp. (Unit 5 at Sect. 10). Sample is 6 cm wide



coralline algae (Fig. 7C) and well-preserved echinoderms. They are terrigenous packstones/grainstones with larger benthic foraminifera (*Heterostegina* and *Amphistegina*), thin-shelled bivalves, bryozoans and nodules of coralline algae and encrusting foraminifera (foralgaliths). Coralline algae belong to the genera *Lithothamnion* sp., *Mesophyllum* sp., *Spongites* sp., and *Lithoporella* sp. Corals only occur as small fragments. Southeast of this section (Fig. 2) the unit comprises terrigenous grainstones with bivalve and echinoid

fragments, benthic foraminifera (Nummulitidae) and branching coralline algae (*Lithothamnion* sp.).

#### 4.6 Unit 6

This is the most extensive and thickest unit, up to 70 m, and consists of alternating conglomerates, sandstones and siltstones. This unit is present in all study sections, except in Sects. 2 and 3 (Figs. 2, 3, 4).

At the base of Sect. 8 (Figs. 2, 4), massive granule to pebble conglomerates, up to 5 m thick, are followed by flat, roughly bedded sandstones and siltstones. Above them, amalgamated channelized deposits, 40–50 cm thick, show fining upward sequences from fine-grained conglomerates to medium/fine sandstones or silty sandstones. These are overlain by horizontal beds of sandstones and silty sandstones, 25–30 cm thick, with occasional bioturbation at the top. Locally, current ripples, 10–15 cm high, and smaller wave ripples appear at the top of the beds. A lobe-shaped morphology of sandstone bodies can be observed at the outcrop scale. Synsedimentary normal faults oriented N120–150E with decimeter-scale throws are common in these beds. These deposits are overlain by a new succession of amalgamated channelized bodies, with fining upward sequences from granule conglomerates to sandstones and silty sandstones, and flat-bedded sandstones.

In the upper part of Sect. 8, clast-supported conglomerates appear in a large channel with erosive base, up to 4–5 m thick and tens of meters wide, which comprises several amalgamated smaller channels with fining-upward sequences, from conglomerate to medium sandstones. Clasts are made of quartzites (mostly), marbles and schists from the Alpujarride basement, mainly from granule (in the matrix) to cobble size (up to 15–20 cm). The axe of this large channel is oriented N25°E. The succession continues with sub-horizontal beds of sandstones and silty sandstones.

Fossil echinoids, as well as internal molds of bivalves and gastropods are locally common in sandstone beds. The bivalves *Lucina dentata* DeFrance, *Lutraria lutraria* (Linnaeus), *Laevicardium oblongum* (Gmelin), *Mactra stultorum* (Linnaeus), *Tellina albicans* Gmelin, *Tellina crassa* Pennant, *Astarte fusca* (Poli), *Pseudoneilonella pusio* (Philippi), *Thracia pubescens* (Pulteney), *Corbula revoluta avitensis* Cossmann & Peyrot, and *Lentidium mediterraneum* (O. G. Costa) have been identified, among other representatives of the orders Lucinoidea, Veneroidea, Carditida, Nuculanida, Anomalodesmata, and Myida unidentifiable at the genus or species levels. Two well-preserved internal molds of the gastropod *Conus* sp. have been found and well-preserved specimens of clypeasteroids were identified as *Clypeaster scillae* Desmoulins and *Clypeaster campanulatus* Schlotheim.

Oyster banks formed by large specimens of *Ostrea edulis* and *Magallana gryphoides* generally occur on top of siltstone and clay beds, although in the upper part of the section they appear within sandstone (Fig. 4). Some of these banks extend laterally for more than 7 m and are up to 50–60 cm thick. Articulated specimens of *O. edulis* are up to 26 cm long, and 18 cm wide, whereas *M. gryphoides* can reach up to 25 cm in length, and 12 cm in width. Locally, buried *Pinna* sp. appears preserved in life position

in silty sandstones. As commented in Unit 4, foraminifera are rare (less than 1% of the residue) and planktonic forms are much scarcer than benthic ones in the siltstones. Among the benthic foraminifera, the species *Anomalinoidea flinti* (Cushman), *Melonis soldanii* (d'Orbigny), *Lenticulina gibba* (d'Orbigny), *Cibicidoides ungerianus* (d'Orbigny), *Marginulina* sp., *Cancris oblongus* (Williamson), *Karreriella bradyi* (Cushman), *Textularia abbreviata* d'Orbigny, *Lenticulina helena* (Karrer), *Bulimina aculeata* d'Orbigny, and *Cibicidoides pseudoungerianus* (Cushman) have been identified. Planktonic foraminifera are represented by *Catapsydrax unicavus* Bolli, Loeblich & Tappan, *Neogloboquadrina acostaensis* (Blow), *Neogloboquadrina pachyderma* (Ehrenberg), and *Dentoglobigerina altispira* (Cushman & Jarvis).

At the top of Unit 6 (Fig. 4), a laterally continuous rudstone bed rich in siliciclastic grains with abundant *O. edulis* and *M. gryphoides* of large size (up to 30 cm) is followed by two rudstone beds, 30 and 70 cm thick, respectively, with a high carbonate content (about 70% CaCO<sub>3</sub>). Both beds are rich in internal molds of Turritellines and clasts of quartzite and marble (Fig. 9). A small rudstone bed, 20 cm thick, with *O. edulis* and *M. gryphoides*, separates the two lower Turritelline beds from a third one of similar characteristics at the top.

This unit also outcrops in isolated patches distributed throughout the valley. In Haza Llana, these patches unconformably overlie all the underlying units (Figs. 2, 3). They consist of massive sandstones and matrix-supported pebble conglomerates with large *O. edulis* and clypeasteroids. In Sect. 6 (Figs. 2, 3), sandstones and fine-grained conglomerates appear at the base, and are followed by strongly cemented sandstone beds, 30–50 cm thick, and large oysters (Fig. 2). In the southern outcrop, in Sect. 12 (Figs. 2, 4), the unit consists of a thick package of siltstones and clays (20–30 m) at the base, followed by sandstones and siltstones, in turn overlain by channelized bodies, decimeters in thickness, of granule to pebble conglomerates intercalated in sandstones. The conglomerates are composed of mainly quartzite clasts in a silty matrix.

## 5 Paleoenvironmental interpretation

### 5.1 Unit 1

The abundance of planktonic foraminifera in the whitish marls in Sect. 3 (Figs. 2, 3, 6B) indicates a pelagic marine environment (Fig. 10A). Benthic foraminifer assemblages point to deep-water conditions. The pelagic marls filled in

**Fig. 9** **A** Rudstone with internal molds of *Turritellines* and clasts of quartzite and dolostone at the top of Unit 6 at Sect. 8. Scale in centimeters. **B** Thin-section micrograph of **A** with *Turritellines* and quartzite and dolostone clasts (sample GUA-TUR)



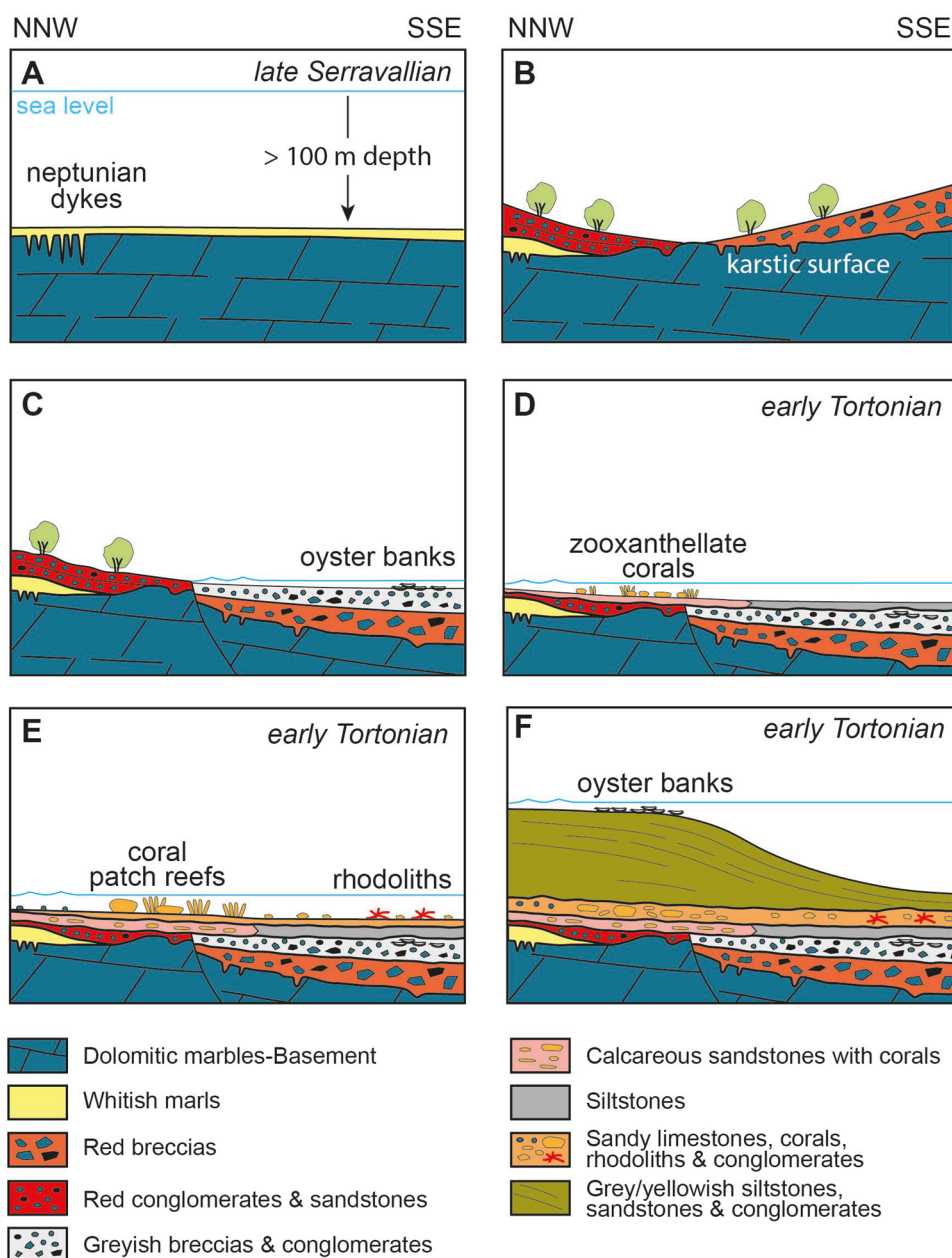
the open fractures (neptunian dykes, Fig. 6A) in the basement, engulfing heterometric, angular clasts derived from the fractured dolomitic marbles with little transport (Fig. 6B). After filling the fractures, the marls draped the seafloor as evidenced by marl beds in Sect. 3 (Figs. 2, 3). Their original thickness and lateral extension cannot be assessed due to subsequent erosion events. Marls of the same age, however, crop out in Hoya de las Bolinas, Zaza ravine (Estévez et al., 1985) and the Ízbor valley (González-Donoso, 1978) (Fig. 1B), suggesting they extended on the Betic basement in a large area.

## 5.2 Unit 2

The subrounded cobbles in a fine-grained matrix in sub-horizontal beds with erosional bases indicate that the red facies of Unit 2 in the Haza Llana area (Fig. 2) correspond to alluvial fan deposits (Fig. 10B). Specifically, they are proximal fan facies where cobbles were transported by turbulent, high-energy and short-lived high-density currents (Colombo, 2010). The alternations of conglomerates and sandstones indicate changes in flow composition during fan progradation.

The heterometric cobble to boulder breccia, with a reddish matrix without fossils of Unit 2 in the rest of the outcrops (Figs. 2, 6C) corresponds to continental foothill deposits (Fig. 10B). This breccia of angular clasts indicates an

**Fig. 10** Paleoenvironmental evolution of the Los Guájares valley area. **A** In the late Serravallian the area was a deep-water pelagic setting. Marls filled in neptunian dykes an extended on the Betic basement. **B** Due to regional uplift the area emerged. Alluvial fans and foothill breccias covered a locally karstified surface. **C** Tectonic restructuring and relative sea-level rise caused partial flooding of the area and formation of near-shore breccias and conglomerates with small oyster banks. **D** In the early Tortonian continued sea-level rise led to shallow-water marine conditions and accumulation of calcareous sandstones with corals and siltstones in deeper settings. **E** Similar environmental conditions prevailed after a tectonic instability that caused an erosive unconformity. Conglomerates, sandy limestones and coral patches formed in the proximal areas, whereas sandy limestones with coralline algae (rhodoliths) prevailed in the more distal southern areas. **F** The marine sedimentation in the Los Guájares valley ended in the early Tortonian with delta deposits with abundant oyster concentrations. Delta-front sediments show a proximal–distal facies trend from north to south



original steep slope at the foot of an Alpujarride paleo-relief (Estévez et al., 1985). It is difficult to establish whether the breccias were more proximal than the alluvial fan facies, since the morphology of basement greatly conditioned the type of deposit. A steep relief would give rise to foothill breccias, whereas a relief with water outflows would promote alluvial fans. Both facies are similar to the Quaternary deposits in the Los Guájares valley and other Betic areas with an Alpujarride bedrock.

### 5.3 Unit 3

Marine bivalves, such as *Chlamys* sp. and bivalve perforations in large angular boulders in the highly heterometric breccia indicate that this is a subtidal deposit formed at a rocky shore with clasts derived by rock fall from the basement with little transport or reworking (Gupta & Allen, 1999) (Fig. 10C). The increase of clast roundness and better sorting of clasts towards the top suggests longer reworking/transport of clasts and a transgressive pattern within the unit. These deposits closely resemble the conglomerates and breccias with perforations found in the Miocene from Sierra Arana-Mencal in the Guadix Basin

(Soria, 1994) and the conglomerates formed at a rocky shoreline of Alpujarride dolostones in the Late Miocene in Sierra de Gádor (Sola et al., 2022) (Fig. 1A). Oysters settled on the conglomerates forming small banks, which were partly reworked by waves.

#### 5.4 Unit 4

The coralline algae *Lithophyllum* sp. and *Neogoniolithon* sp. (Aguirre et al., 2017; Braga, 2017; Braga et al., 2010), and the hermatypic corals *Porites* and *Tarbellastraea* suggest that calcareous sandstones were deposited in shallow subtidal environments (Fig. 10D). These coral genera formed reef structures of diverse dimensions, from meters to tens of meters in width, and decimeters to meters in thickness, in shallow paleoenvironments with terrigenous influx during the Late Miocene in the Neogene Betic basins (Braga et al., 1990; Martín et al., 1989; Santisteban & Taberner, 1983). In addition, the depositional setting was of low/moderate energy due to the presence of abundant micritic matrix. Hermatypic corals are typical of warm waters, in which lowest mean temperatures are higher than 16 °C (Veron, 1995). Applying the “energy hypothesis” of Fraser and Currie (1996), the genus richness during the Tortonian suggests minimum sea-surface temperatures of about 18 °C in the Mediterranean (Bosellini & Perrin, 2008; Rosen, 1999). In Unit 4, the small size of colonies points to a stressed environment with frequent disturbances limiting the coral growth (Bauman et al., 2013; Vermeij et al., 2007). These calcareous sandstones change laterally to silts formed in lower-energy, deeper settings, as already pointed out by Estévez et al. (1985).

#### 5.5 Unit 5

Unit 5 has biogenic components similar to those of Unit 4. It also accumulated in shallow-water settings in which zooanthellate corals grew under the influence of terrigenous sedimentation in a generally low-energy environment as evidenced by the common occurrence of fine-grained sediment among the coral colonies and patches (Figs. 4, 8A, 10E). The presence of *Hyotissa hyotis* in Sect. 10 (Figs. 2, 4) is typical of warm-water reef environments and this species mainly inhabits shallow settings (Freneix et al., 1988). The occurrence of planktonic foraminifera suggests that the environment was open to the ocean.

The conglomerate of subangular pebbles with a packstone matrix in Sect. 4 in the Haza Llana area (Figs. 2, 3) can be interpreted as a more proximal and higher-energy facies than those outcropping around Guájar-Faragüit. The mixture of bioclastic components and reworked rock fragments derived from the Alpujarride suggest that the conglomerate formed in a rocky shore at the basin margin (Betzler et al., 1997;

Sola et al., 2022). In contrast, the branching coralline alga *Lithothamnion* and the foralgaliths composed of encrusting foraminifera and *Lithothamnion* and *Mesophyllum* in the sandy limestones at the southern outcrops (Sect. 12, Figs. 2, 4, 7C) indicate more distal paleoenvironments, several tens of meters deep (Aguirre et al., 2017; Bosence, 1991; Braga, 2017; Prager & Ginsburg, 1989).

#### 5.6 Unit 6

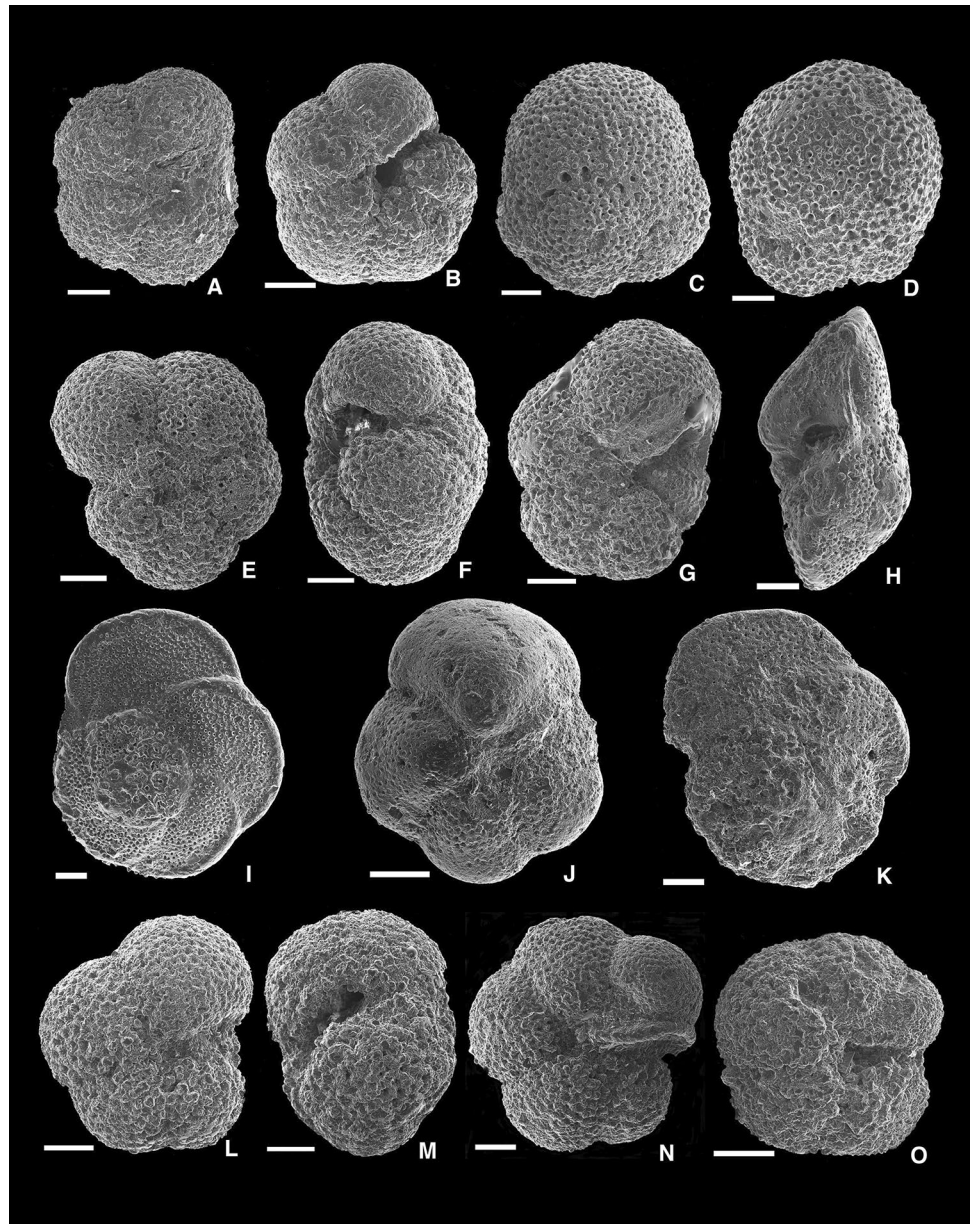
Sediments in Unit 6 show lithologies, structures and fossil components characteristic of a fine-grained, fluvial dominated delta (Fig. 10F). Numerous channels occur at various levels within the unit, displaying fining-upward sequences from gravel to silt. The ripples that appear at some levels indicate a moderate influence of wave action. The facies association of this deltaic system indicates a delta front area, with a combination of channels and sand lobes with small interdistributary bays where silts predominated (Rodríguez-López & Arche, 2010). The banks of *M. gryphoides* that occur in the silty beds throughout the unit can be associated with interdistributary areas (Aguirre, 1998; Demarcq & Demarcq, 1989, 1990; Littlewood & Donovan, 1988; Martinius, 1991; Stenzel, 1971) where they lived attached to one another to counteract the adverse conditions presented by this type of environment (Herb & Geister, 1984). *O. edulis* and *M. gryphoides* are euryhaline bivalves that live in shallow marine environments (less than 20–30 m depth) and in hypersaline to brackish waters. The great abundance of oysters and the large size they reach in this unit would indicate a high productivity in the environment (Wood, 1993). The dense concentrations of Turritellinae (Fig. 9) at the top of the unit are also indicative of high nutrient content, usually showing an abundance of phytoplankton (Allmon & Knight, 1993; Allmon, 1988, 1992). The river was probably the nutrient source for the environment. The generally fine-grained nature of the sediments and the high nutrient levels indicated by the fossil assemblages suggest that the fluvial system feeding the delta was perennial.

Facies distribution in the valley gives some indication of proximal/distal patterns. The predominance of sands and silts with small channels at Sect. 12 (Figs. 2, 4) suggests that the deposits in the southern outcrop are the most distal ones.

## 6 Age of the stratigraphic units

Estévez et al. (1985) were not able to obtain planktonic foraminifera from the samples collected in the Los Guájares valley. In the samples of Unit 1 in the Haza Llana area (Figs. 2, 3), the planktonic foraminifera are very scarce, including *Globigerina* spp., *Globigerinita glutinata*, *Paragloborotalia mayeri*, *P. continuosa*, *P. siakensis*, and

**Fig. 11** Biostratigraphically significant planktonic foraminifer species in the study samples. **A** *Paragloborotalia continuosa*, umbilical view. Unit 1, Haza Llana area (sample MG-1b). **B** *Paragloborotalia siakensis*, umbilical view. Unit 1, Haza Llana area (sample MG-1b). **C** *Orbulina suturalis*, Unit 1, Haza Llana area (sample MG-1b). **D** *Orbulina suturalis*, Unit 1, Zaza ravine (sample PdV\_M0). **E** *Paragloborotalia siakensis*, spiral view. Unit 1, Zaza ravine (sample PdV\_M0). **F** *Paragloborotalia siakensis*, peripheral view. Unit 1, Zaza ravine (sample PdV\_M0). **G** *Paragloborotalia mayeri*, umbilical view. Unit 1, Zaza ravine (sample PdV\_M0). **H** *Globorotalia praemenardii*, peripheral view. Unit 1, Zaza ravine (sample PdV\_M0). **I** *Globorotalia menardii*, spiral view. Unit 1, Zaza ravine (sample PdV\_M0). **J** *Globorotalia praescitula-scitula*, umbilical view. Unit 1, Hoya de las Bolinas (sample LLDS\_M1). **K** *Globorotalia praemenardii*, spiral view. Unit 1, Hoya de las Bolinas (sample LLDS\_M1). **L–M** *Paragloborotalia continuosa*, umbilical (L) and peripheral (M) views. Unit 4 (sample MG-4b). **N–O** *Neogloboquadrina acostaensis*, umbilical views. Unit 6 (sample MG-6 k). Scale bars: 50  $\mu$ m



*Orbulina suturalis* (Fig. 11A–C). This species assemblage ranges from the late Langhian to the earliest Tortonian (Wade et al., 2011; Young et al., 2017). Whitish marls, similar to those of Unit 1 from the Haza Llana area (Fig. 2), crop out in the nearby Zaza ravine, about 4 km to the NE, by the road connecting Los Guájares with Pinos del Valle (Fig. 1B). Estévez et al. (1985) indicated that the age of these marls was inconclusive as they found two groups of species of different age, which appear in similar state of preservation: one indicating a basal Serravallian and another pointing to a middle Serravallian age. However, they favored a basal Serravallian age, as the most consistent and simplest hypothesis (Estévez et al., 1985).

We collected a sample of whitish marls in the Zaza ravine to test their age and the possible correlation with the whitish marls of Unit 1. This sample is rich in planktonic foraminifera, with the following assemblage: *Paragloborotalia siakensis* (very abundant), *P. mayeri* (very abundant), *Globorotalia menardii*, *G. praemenardii*, *G. scitula*, *Dentoglobigerina altispira*, *Sphaeroidinellopsis* spp., *Orbulina universa*, *O. suturalis*, *Trilobatus trilobus*, *Globigerinoides obliquus*, and *Globigerina bulloides* (Fig. 11D–I). The last appearance of *G. praemenardii* and the first occurrence of *G. menardii* occurred between 11.97 and 13.41 Ma, late Serravallian (Young et al., 2017), postdating the age attributed by Estévez et al. (1985).

Three marl samples, stratigraphically located between the metamorphic basement and reddish conglomerates equivalent to Unit 2, were also collected at the base of the Miocene succession in the Ízbor valley (Fig. 1B) that was previously studied by González-Donoso (1978). The sampling locality is 8 km to the northeast of the Haza Llana outcrops, now at the exit 167 of the motorway A-44. Specimens of *P. mayeri*, *P. siakensis*, *Globorotalia praescitula-scitula*, *G. praemenardii*, *G. menardii*, and *Fohsella fohsi* were identified in these marls. This assemblage also indicates a late Serravallian age.

Two additional samples were collected in greenish marls cropping out in Hoya de las Bolinas, 4–5 km northeast of Guájar-Faragüit (Fig. 1B). They contain late Serravallian planktonic foraminifera assemblages similar to those in the Zaza ravine, dominated by *Globigerinoides* spp., *Globigerina* spp., *Sphaeroidinellopsis* spp., *P. siakensis*, *P. mayeri*, *G. praemenardii*, and *G. scitula-praescitula* (Fig. 11J, K). In summary, the more precise constraint provided by foraminifer assemblages from nearby localities suggests a late Serravallian age for the marls in Unit 1.

The planktonic foraminifera found in the silts of Unit 4 (*Catapsydrax unicavus*, *Globigerina bulloides*, *Globigerinita glutinata*, *Orbulina suturalis*, and *Paragloborotalia continuosa*) (Fig. 11L, M) indicate a wide age range, from the middle Langhian (first occurrence of *O. suturalis*) to the earliest Tortonian (last occurrence of *C. unicavus*) (Wade et al., 2011; Young et al., 2017). Taking into consideration the stratigraphic position of Unit 4, well above the late Serravallian marls of Unit 1, it seems reasonable to assume an earliest Tortonian age for this unit.

In Unit 6, the presence of *Catapsydrax unicavus*, *Neogloboquadrina pachyderma*, and *N. acostaensis* (Fig. 11N, O), together with the lack of late Tortonian species, indicates an early Tortonian age (Wade et al., 2011; Young et al., 2017).

## 7 Discussion

### 7.1 Sedimentary and paleogeographic evolution

The Miocene deposits in the Los Guájares valley reflect dramatic changes in depositional environments from deep marine to continental, which reveal a series of tectonic movements of the region, also recorded by the unconformities separating the distinguished units. Following the exhumation of the Alpujarride Complex after burial high-pressure metamorphism (Azañón et al., 1998), in the late Serravallian the Los Guájares Nappe was exposed at the sea floor in a deep pelagic environment. The marls of Unit 1 filled in open fractures in the basement, which indicate a local extensional context, compatible with the extensional context that has been described in the entire Betic basement

in the Serravallian (Comas et al., 1992; Galindo-Zaldívar et al., 2019; Martínez-Martos et al., 2017). Marls of Unit 1 extended over the Alpujarride basement from Los Guájares valley to the Zaza ravine and Hoya de las Bolinas (Fig. 1B). Similar marls rich in planktonic foraminifera of Serravallian age were described by González-Donoso (1978) overlying Alpujarride schists in the Ízbor valley (Fig. 1B). These marls were interpreted as coastal lagoon deposits by Rustichelli et al. (2013) due to the occurrence of gypsum in them. Nonetheless, the gypsum in the marls is secondary gypsum filling fractures and it is probably derived from the Alpujarride basement. In addition, the marls contain abundant planktonic foraminifera, indicating that they are pelagic sediments similar to those in Unit 1.

The exposure of at least part of the Alpujarride basement on the sea floor, however, took place earlier in the Early Miocene (early Burdigalian). In the southern part of the Granada Basin, near Murchas (Fig. 1), the Alpujarride basement is overlain by pelagic sediments older than those of the Los Guájares valley. González-Donoso (1978) and Rodríguez-Fernández (1982) described lower Burdigalian marls overlying a breccia of clasts derived from the underlying Alpujarride basement. A similar succession of breccia of basement clasts and marls rich in early Burdigalian planktonic foraminifera was described as the Alamillos Formation by Rodríguez-Fernández (1982) at the base of the Neogene deposits in the Guadix Basin (Fig. 1A). Pascual-Molina (1997) reported pelagic deposits late Burdigalian-early Langhian in age on the Betic basement at the northwestern margin of Sierra Alhamilla and open-marine sediments rich in middle-Burdigalian planktonic foraminifera overlie Maláguide and Alpujarride rocks north of Sierra Cabrera and south of Sierra de Almagro at the margins of the Sorbas and Vera basins, respectively (Hodgson, 2002; Rondeel, 1965; Völk, 1967) (Fig. 1A).

The basement uplift continued and led to emersion of the area, reflected in the continental foothill breccias and alluvial fan sediments of Unit 2. Similar fluvial deposits can be found in the southern part of the Granada Basin, the so-called “limos rojos de Albuñuelas” -Albuñuelas red silts- (González-Donoso, 1978), and above the Serravallian marls rich in planktonic foraminifera in the Ízbor valley outcrop (González-Donoso, 1978; Rustichelli et al., 2013) (Fig. 1B). These red conglomerates, sandstones and siltstones have been considered Serravallian in age due to their micromammal fossils (Martín-Suárez et al., 1993) as well as their stratigraphic position above the Serravallian marls (González-Donoso, 1978). Red conglomerates, sandstones and silts attributed to a Serravallian-early Tortonian age occur around Sierra Nevada (basal member of La Peza Formation, Rodríguez-Fernández, 1982; Rodríguez-Fernández et al., 1990), in the Tabernas, Sorbas and Vera basins, south



and southeast of Sierra de Filabres, extending southwards to the Sierras de la Contraviesa, Gádor, Alhamilla and Cabrera (Barragán, 1997; Doyle et al., 1996; Kleverlaan, 1989; Montenat, 1990; Rondeel, 1965) (Fig. 1A). In the Poniente Basin at the southern slopes of Sierra de Gádor (Almería, SE Spain) (Fig. 1A), red conglomerates, sandstones and silts change upwards to shallow-marine deposits including an ash layer dated at  $12.3 \pm 0.6$  Ma (latest Serravallian) (Sola et al., 2013). North of Sierra de Filabres, red siliciclastic deposits extend to the Sierra de las Estancias (Braga & Martín, 1988) and Sierra de Baza (Soria, 1993) (Fig. 1A). All these continental deposits indicate the existence of a large emergent Betic upland (Braga et al., 2003).

The Los Guájares area was submerged again and became a shallow-water marine setting during deposition of Units 3 to 6. There were areas in the Betic basement that continued to rise, such as the antecedent reliefs of the present-day Sierra de la Tórtola or the Sierra Nevada nucleus (Braga et al., 2003) (Fig. 1A), while other areas such as the present-day Los Guájares valley were flooded by a relative sea-level rise. The grey breccias and conglomerates of Unit 3 formed at a rocky shoreline witnessing the initial steps of the flooding.

Further relative sea-level rise led to the establishment of a shallow marine environment with terrigenous influx from emergent reliefs in the early Tortonian during accumulation of Units 4 and 5, in which coral reefs thrived building small structures. Tectonic instability generated an erosive unconformity between Units 4 and 5 but the depositional paleoenvironment did not substantially change from one unit to the other. Some synsedimentary normal faults can be observed cutting deposits of these two units, which probably contributed to the creation of accommodation and reflect the extensional tectonics that generated the compartmentalization of the region mentioned above. Shallow-water deposits including small coral patches early Tortonian in age also occur in the southern part of the Granada Basin, near Albuñuelas (Juncal, Rivas et al., 1999) (Fig. 1B). These corals grew on conglomerates fed from the antecedent relief of the Sierra de la Tórtola, located to the north (Fig. 1A).

The nearshore, shallow-water marine conditions continued with the installation of a delta system in the area, mainly recorded by delta front deposits. The total thickness of the deposits, about 70 m, suggests a moderate subsidence to keep accommodation to similar delta-front facies during all the succession of Unit 6. The change from a carbonate-dominated setting to a terrigenous system might indicate higher sediment input due to increased uplift rate of the emergent source uplands. The presumably perennial nature of the fluvial system suggests a period of more humid climatic conditions at the southern slopes of the antecedent relief of Sierra de la Tórtola-Sierra Nevada (Fig. 1A) during the early Tortonian. This interpretation, however, is not supported by the

early Tortonian pollen records in the southern Iberian Peninsula, which indicate a vegetation dominated by herbs and shrubs characteristic of relatively arid scrublands (Jiménez-Moreno et al., 2010). The occurrence of coeval fine-grained siliciclastic deposits rich in Turritellinae and oyster banks, immediately south of Sierra de la Tórtola (Rivas et al., 1999) (Fig. 1), suggests a certain areal extension of shallow-marine environments with high nutrient levels.

The complete and permanent emersion of the area took place since the early Tortonian, with intense deformation by folding and faulting that affected the Miocene rocks (Avidad et al., 1978; Estévez et al., 1985; Sanz de Galdeano & López-Garrido, 2000). The most common faults are roughly NW–SE normal faults, which also occur at the transition from the Granada Basin to Sierra Nevada (Fig. 1), facilitating an ENE–WSW extension and the relative subsidence of the basin and uplift of the mountain range (Galindo-Zaldívar et al., 2019). The end of marine sedimentation and emergence of Los Guájares is coeval with the individualization of the Granada Basin under a geodynamic regime determined by NNW–SSE to N–S compression. Sierra Nevada, Sierra de la Tórtola and the Betic basement to the south (Fig. 1A) were folded forming large E–W antiforms (Avidad et al., 1978; Galindo-Zaldívar et al., 2019; Sanz de Galdeano & Alfaro, 2004).

Shallow-marine sedimentation continued to the north and east of Los Guájares valley, with deposition of terrigenous rudstones to packstones, unconformably overlying the Betic basement and older Miocene deposits (Avidad et al., 1978; Braga et al., 1996; Estévez et al., 1985; González-Donoso, 1978; Rodríguez-Fernández, 1982; Rustichelli et al., 2013). These limestones extend southward to the Ízbor valley section (Fig. 1B) and probably are the remnants of the connection of the Granada Basin with the Mediterranean Sea during the Tortonian. Overlying these limestones, upper Tortonian coral reefs and delta systems were the last marine deposits in the Granada Basin before its isolation from the open sea by the end of the Tortonian (Braga et al., 1990; Dabrio et al., 1982; Galindo-Zaldívar et al., 2019; García-Alix et al., 2008).

Quaternary deposits are scattered throughout the valley and surrounding areas at the foot of the reliefs.

## 7.2 Coral reefs in the context of the western Mediterranean

The isolated small coral colonies and the coral colonies building the small coral patches in Units 4 and 5 mainly belong to *Tarbellastraea* and *Porites*. Only one colony of *Thegiostraea* was found. Coral heads of *Tarbellastraea* and *Porites* intensely bored by bivalves were also reported in lower Tortonian deposits in the vicinity of Albuñuelas (Juncal, Rivas et al., 1999), about 10 km NW of the Los Guájares

reefs (Fig. 1B). These are the only coral reefs confidently dated as early Tortonian known in the Betic Cordillera. The genus richness in these reefs is lower than the one in older Langhian reefs in the Granada Basin, in which 8 genera were reported (Braga et al., 1996), and lower than the richness in late Tortonian reefs, which comprise 7 genera in the Almanzora Corridor (Martín et al., 1989) (Fig. 1A). Both assemblages include the three genera found in Los Guájares. The lower genus richness of coral reefs in the early Tortonian is probably due to a sampling bias caused by the limited extension of outcrops with reefs from this age, although unfavorable conditions for reef development cannot be ruled out. In this regard, in the entire Mediterranean region, zooxanthellate corals of early Tortonian (and Serravallian?) age have only been reported in detritic facies in the Rhône Valley. They consist of isolated colonies of *Tarbellastraea* and *Montastraea* that did not build reefs (Chevalier & Demarq, 1964; Perrin & Bosellini, 2012). By contrast, upper Tortonian reefs have been described in tens of localities all over the Mediterranean (Perrin & Bosellini, 2012). This scarcity of records and the very low diversity in the known localities might be an artifact due to the difficulty of assigning a precise age to Upper Miocene shallow-water carbonates. It might be possible that some early Tortonian coral reefs or zooxanthellate-coral sites were considered late Tortonian in age just because these structures and fossils are more common in the latter interval. However, the very low number of records suggests a true rarity of zooxanthellate corals during the early Tortonian in the Mediterranean region. The global conditions in the early Tortonian were not favorable for coral reef development as the sea level fell more than 30 m in that interval and global temperatures were 3–4 °C cooler than in times before the Middle Miocene Climatic Transition (Miller et al., 2020; Perrin & Bosellini, 2012). This cooling is also reflected in the pollen records of the southern Iberian Peninsula with a decrease in thermophilus plants (Jiménez-Moreno et al., 2010). In the case of the Mediterranean, these unfavorable circumstances affected a zooxanthellate coral fauna already isolated from the Indo-Pacific and consequently with a limited genetic pool (Perrin & Bosellini, 2012, 2013).

## 8 Conclusions

Miocene rocks occur in the Los Guájares valley, about 35 km south of Granada, in small and tectonized outcrops on metamorphic rocks of the Alpujarride Complex of the Internal Zones of the Betic Cordillera.

Six sedimentary units separated by unconformities were distinguished by mapping and logging the Miocene deposits. The lowest unit consists of upper Serravallian marls

with planktonic foraminifera filling neptunian dykes and draping the Alpujarride dolomitic marbles. They are deep pelagic deposits formed on the basement under an extensional regime. The overlying red conglomerates and breccias indicate continental deposition after emersion of the region. These materials are roughly coeval of other continental deposits that extend over the Betic basement in the central and eastern sectors of the cordillera. Relative sea-level rise and marine flooding of the area are evidenced by grey conglomerates with marine fossils in the following unit. Shallow marine conditions continued during deposition of the next two units in the early Tortonian, as indicated by coralline algae, zooxanthellate corals and small coral reefs included in sandstones and sandy limestones. The last marine Miocene rocks are delta front deposits early Tortonian in age. The lithology and facies distribution suggest a proximal–distal gradient from north to south. The abundance of oyster banks and concentrations of Turritellines point to a paleoenvironment with high nutrient levels.

The Los Guájares area emerged after the early Tortonian. Basement and Miocene deposits were folded and faulted under NNW–SSE to N–S compression and erosion processes prevailed in the valley.

The coral patches in Los Guájares, together with the nearby coral heads in Albuñuelas are the only documented early Tortonian coral reefs in the Mediterranean region.

**Acknowledgements** This work was supported by the Ministerio de Ciencia, Innovación y Universidades, Spain, project PGC2018-099391-B-I00 and Junta de Andalucía Research Group RNM 190. We are grateful to Hugo Corbí and an anonymous reviewer for their comments that helped to improve a previous version of this paper. We also acknowledge Jodi Eckart for the English editing.

**Funding** Funding for open access publishing: Universidad de Granada/CBUA.

**Data availability statement** All authors contributed to the study conception and design. All data supporting the findings of this study are available within this paper. All authors read and approved the final manuscript.

## Declarations

**Conflict of interest** We declare that they have no conflicts of interest between themselves and the research being submitted for publication in the journal.

**Open Access** This article is licensed under a Creative Commons Attribution 4.0 International License, which permits use, sharing, adaptation, distribution and reproduction in any medium or format, as long as you give appropriate credit to the original author(s) and the source, provide a link to the Creative Commons licence, and indicate if changes were made. The images or other third party material in this article are included in the article's Creative Commons licence, unless indicated otherwise in a credit line to the material. If material is not included in the article's Creative Commons licence and your intended use is not permitted by statutory regulation or exceeds the permitted use, you will

need to obtain permission directly from the copyright holder. To view a copy of this licence, visit <http://creativecommons.org/licenses/by/4.0/>.

## References

- Aguirre, J. (1998). Bioconstrucciones de *Saccostrea cucullata* Born, 1778 en el Plioceno superior de Cádiz (SO de España): Implicaciones paleoambientales y paleoclimáticas. *Revista Española De Paleontología*, 13(1), 27–36. <https://doi.org/10.7203/sjp.23969>
- Aguirre, J., Braga, J. C., & Bassi, D. (2017). Rhodoliths and rhodolith beds in the rock record. In R. Riosmena-Rodríguez, W. Nelson, & J. Aguirre (Eds.), *Rhodolith/maërl beds: A global perspective* (pp. 105–138). Springer International Publishing, Geerbestrasse, Switzerland. [https://doi.org/10.1007/978-3-319-29315-8\\_5](https://doi.org/10.1007/978-3-319-29315-8_5)
- Allmon, W. D. (1988). Ecology of recent turrilline gastropods (Prosobranchia, Turritellidae): Current knowledge and paleontological implications. *Palaïos*, 3(3), 259–284. <https://doi.org/10.2307/3514657>
- Allmon, W. D. (1992). Role of temperature and nutrients in extinction of turrilline gastropods: Cenozoic of northwestern Atlantic and northeastern Pacific. *Palaeogeography, Palaeoclimatology, Palaeoecology*, 92(1–2), 41–54. [https://doi.org/10.1016/0031-0182\(92\)90134-Q](https://doi.org/10.1016/0031-0182(92)90134-Q)
- Allmon, W. D., & Knight, J. L. (1993). Paleocological significance of turrilline gastropod-dominated assemblage in the Cretaceous of South Carolina. *Journal of Paleontology*, 67(3), 355–360. <https://doi.org/10.1017/S0022336000036830>
- Avidad, J., García-Dueñas, V., Gallegos, J. A., & González-Donoso, J. M. (1978). *Mapa geológico de la Hoja nº 1041 (Dúrcal). Mapa Geológico de España E. 1:50.000. Segunda Serie (MAGNA)*, Primera edición. IGME.
- Azañón, J. M., García-Dueñas, V., & Goffé, B. (1998). Exhumation of high-pressure metapelites and coeval crustal extension in the Alpujarride complex (Betic Cordillera). *Tectonophysics*, 285(3), 231–252. [https://doi.org/10.1016/S0040-1951\(97\)00273-4](https://doi.org/10.1016/S0040-1951(97)00273-4)
- Barragán, G. (1997). *Evolución geodinámica de la Depresión de Vera. Provincia de Almería. Cordilleras Béticas*. Ph.D. Thesis, Univ. Granada, Spain.
- Bauman, A. G., Pratchett, M. S., Baird, A. H., Riegl, B., Heron, S., & Feary, D. A. (2013). Variation in the size structure of corals is related to environmental extremes in the Persian Gulf. *Marine Environmental Research*, 84, 43–50. <https://doi.org/10.1016/j.marenvres.2012.11.007>
- Betzler, C., Brachert, T. C., Braga, J. C., & Martín, J. M. (1997). Nearshore, temperate, carbonate depositional systems (lower Tortonian, Agua Amarga Basin, southern Spain): Implications for carbonate sequence stratigraphy. *Sedimentary Geology*, 113(1–2), 27–53. [https://doi.org/10.1016/S0037-0738\(97\)00054-7](https://doi.org/10.1016/S0037-0738(97)00054-7)
- Bosellini, F. R., & Perrin, C. (2008). Estimating Mediterranean Oligocene-Miocene sea surface temperatures: An approach based on coral taxonomic richness. *Palaeogeography, Palaeoclimatology, Palaeoecology*, 258(1–2), 71–88. <https://doi.org/10.1016/j.palaeo.2007.10.028>
- Bosence, D. W. J. (1991). Coralline algae: Mineralization, taxonomy, and palaeoecology. In R. Riding (Ed.), *Calcareous algae and stromatolites* (pp. 98–113). Springer, Berlin, Heidelberg. [https://doi.org/10.1007/978-3-642-52335-9\\_5](https://doi.org/10.1007/978-3-642-52335-9_5)
- Braga, J. C. (2017). Neogene rhodoliths in the Mediterranean basins. In R. Riosmena-Rodríguez, W. Nelson, & J. Aguirre (Eds.), *Rhodolith/maërl beds: A global perspective* (pp. 169–193). Springer.
- Braga, J. C., & Martín, J. M. (1988). Neogene coralline-algal growth-forms and their palaeoenvironments in the Almanzora river valley (Almería, S.E. Spain). *Palaeogeography, Palaeoclimatology, Palaeoecology*, 67(3), 285–303. [https://doi.org/10.1016/0031-0182\(88\)90157-5](https://doi.org/10.1016/0031-0182(88)90157-5)
- Braga, J. C., Martín, J. M., & Alcalá, B. (1990). Coral reefs in coarse-terrigenous sedimentary environments (Upper Tortonian, Granada Basin, southern Spain). *Sedimentary Geology*, 66(1–2), 135–150. [https://doi.org/10.1016/0037-0738\(90\)90011-H](https://doi.org/10.1016/0037-0738(90)90011-H)
- Braga, J. C., Jiménez, A. P., Martín, J. M., & Rivas, P. (1996). Middle Miocene coral-oyster reefs, Murchas, Granada, southern Spain. In E. K. Franseen, M. Esteban, W. C. Ward, & J. M. Rouchy (Eds.), *Models for carbonate stratigraphy from Miocene reef complexes of Mediterranean regions* (vol. 5., pp. 131–139). SEPM Concepts in Sedimentology and Paleontology, Tulsa. <https://doi.org/10.2110/csp.96.01.0131>
- Braga, J. C., Martín, J. M., & Quesada, C. (2003). Patterns and average rates of late Neogene-Recent uplift of the Betic Cordillera SE Spain. *Geomorphology*, 50(1), 3–26. [https://doi.org/10.1016/S0169-555X\(02\)00205-2](https://doi.org/10.1016/S0169-555X(02)00205-2)
- Braga, J. C., Bassi, D., Piller, W. E., 2010. Palaeoenvironmental significance of Oligocene-Miocene coralline red algae - a review. In M. Mutti, W. E. Piller & C. Betzler, (Eds.), *Carbonate systems during the Oligocene-Miocene climatic transition* (pp. 165–182). International Association of Sedimentologists Special Publication 42.
- Chevalier, J. P., & Demarq, G. (1964). Les madréporaires miocènes de la vallée du Rhône. *Travaux des Laboratoires de Géologie de la Faculté des Sciences de Lyon, Nouvelle Série*, 11, 7–48.
- Colombo, F. (2010). Abanicos aluviales: procesos de transporte y acumulación de materiales detríticos. In A. Arche (Ed.), *Sedimentología. Del proceso físico a la cuenca sedimentaria*. Consejo Superior de Investigaciones Científicas, Madrid, 85–130.
- Comas, M. C., García-Dueñas, V., & Jurado, M. J. (1992). Neogene tectonic evolution of the Alboran Sea from MCS data. *Geo-Marine Letters*, 12(2), 157–164. <https://doi.org/10.1007/BF02084927>
- Dabrio, C. J., Martín, J. M., & Megías, A. G. (1982). Signification sédimentaire des évaporites de la depression de Grenade (Espagne). *Bulletin de la Societé Géologique de France*, 24(4), 705–710. <https://doi.org/10.2113/gssgfbull.S7-XXIV.4.705>
- Delgado, F., Estévez, A., Martín, J. M., & Martín-Algarra, A. (1981). Observaciones sobre la estratigrafía de la formación carbonatada de los mantos alpujarrides (Cordilleras Béticas). *Estudios Geológicos*, 37(1–2), 45–57.
- Demarcq, G., & Demarcq, H. (1989). Biostrome à *Crassostrea* du Quaternaire récent (Sénégal), comparaison avec ceux du Miocène (bassin Rhodanien). *Géologie Méditerranéenne*, 16(1), 3–15. [https://doi.org/10.1016/S0016-6995\(06\)80401-8](https://doi.org/10.1016/S0016-6995(06)80401-8)
- Demarcq, G., & Demarcq, H. (1990). Découverte d'un biostrome récent à *Crassostrea* (Bivalves) dans une mangrove du Sénégal. *Comptes rendus de l'Académie des sciences. Série 2, Mécanique, Physique, Chimie, Sciences de l'univers, Sciences de la Terre*, 310(5), 651–654.
- Doyle, P., Mather, A. E., Bennet, M. R., & Bussell, M. A. (1996). Miocene barnacle assemblages from southern Spain and their palaeoenvironmental significance. *Lethaia*, 29(3), 267–274. <https://doi.org/10.1111/j.1502-3931.1996.tb01659.x>
- Estévez, A., González-Donoso, J. M., Linares, A. C., Garrido, A., Rodríguez-Fernández, J., Sanz de Galdeano, C., & Serrano, F. (1985). El Neógeno del Valle de Los Guájares (Cordillera Bética, Granada). *Mediterránea: Serie de Estudios Geológicos*, 4, 33–54.
- Fallot, P. (1948). Les Cordilleres Betiques. *Estudios Geológicos*, 8, 83–112.
- Fraser, R. H., & Currie, D. J. (1996). The species richness-energy hypothesis in a system where historical factors are thought to

- prevail: Coral reefs. *The American Naturalist*, 148(1), 138–159. <https://doi.org/10.1086/285915>
- Freneix, S., Saint-Martin, J. P., & Moissette, P. (1988). Huîtres du Messinien d'Oranie (Algérie occidentale) et paléobiologie de l'ensemble de la faune de bivalves. *Bulletin Du Muséum National D'histoire Naturelle*, 10(4), 1–21.
- Galindo-Zaldívar, J., Braga, J. C., Marín-Lechado, C., Ercilla, G., Martín, J. M., Pedrera, A., Casas, D., Aguirre, J., Ruiz-Constán, A., Estrada, F., & Puga-Bernabéu, Á. (2019). Extension in the Western Mediterranean. In C. Quesada, & J. Oliveira (Eds.), *The geology of Iberia: A geodynamic approach: Volume 4: Cenozoic basins* (pp. 61–103). Springer International Publishing. [https://doi.org/10.1007/978-3-030-11190-8\\_3](https://doi.org/10.1007/978-3-030-11190-8_3)
- García-Alix, A., Minwer-Barakat, R., Martín, J. M., Suárez, E. M., & Freudenthal, M. (2008). Biostratigraphy and sedimentary evolution of Late Miocene and Pliocene continental deposits of the Granada Basin (southern Spain). *Lethaia*, 41(4), 431–446. <https://doi.org/10.1111/j.1502-3931.2008.00097.x>
- García-Hernández, M., López-Garrido, A. C., Rivas, P., Sanz de Galdeano, C., & Vera, J. A. (1980). Mesozoic paleogeographic evolution in the External Zones of the Betic Cordillera (Spain). *Geologie En Mijnbouw*, 59(2), 155–168.
- Gómez-Pugnaire, M. T., Braga, J. C., Martín, J. M., Sassi, F. P., & Del Moro, A. (2000). Regional implications of a Palaeozoic age for the Nevado-Filabride Cover of the Betic Cordillera. *Spain. Schweizerische Mineralogische Und Petrographische Mitteilungen*, 80(1), 45–52.
- Gómez-Pugnaire, M. T., Galindo-Zaldívar, J., Rubatto, D., González-Lodeiro, F., Sánchez-Vizcaino, V. L., & Jabaloy, A. (2004). A reinterpretation of the Nevado-Filabride and Alpujarride Complexes (Betic Cordillera): Field, petrography and U-Pb ages from orthogneisses (western Sierra Nevada, S Spain). *Schweizerische Mineralogische Und Petrographische Mitteilungen*, 84, 303–322.
- González-Donoso, J. M. (1978). Los materiales miocénicos de la Depresión de Granada. *Cuadernos De Geología, Universidad De Granada*, 8–9, 191–204.
- Gupta, S., & Allen, P. A. (1999). Fossil shore platforms and drowned gravel beaches; evidence for high-frequency sea-level fluctuations in the distal Alpine foreland basin. *Journal of Sedimentary Research*, 69(2), 394–413. <https://doi.org/10.2110/jsr.69.394>
- Herb, R., & Geister, J. (1984). Récifs à huîtres récents et Miocènes. In J. Geister, & R. Herb (Eds.), *Géologie et paléoécologie des récifs*. Institut de Géologie de l'Université de Berne, 22.1–22.12.
- Hodgson, D. M. (2002). *Tectono-stratigraphic evolution of a Neogene oblique extensional orogenic basin, southeast Spain*. Ph.D. Thesis, University of London.
- Jiménez-Moreno, G., Suc, J. P., & Fauquette, S. (2010). Miocene to Pliocene vegetation reconstruction and climate estimates in the Iberian Peninsula from pollen data. *Review of Palaeobotany and Palynology*, 162(3), 403–415. <https://doi.org/10.1016/j.revpalbo.2009.08.001>
- Johnson, B. J., Fogel, M. L., & Miller, G. H. (1998). Stable isotopes in modern ostrich eggshell: A calibration for paleoenvironmental applications in semi-arid regions of southern Africa. *Geochimica Et Cosmochimica Acta*, 62(14), 2451–2461. [https://doi.org/10.1016/S0016-7037\(98\)00175-6](https://doi.org/10.1016/S0016-7037(98)00175-6)
- Kleverlaan, K., 1989. *Tabernas fan complex. A study of a Tortonian fan complex in a Neogene basin, Tabernas, Province of Almería, SE Spain*. Ph.D. Thesis, University of Amsterdam, The Netherlands, 97 pp.
- Littlewood, D. J., & Donovan, S. K. (1988). Variation of recent and fossil *Crassostrea* in Jamaica. *Palaeontology*, 31(4), 1013–1028.
- Lonergan, L. (1993). Timing and kinematics of deformation in the Malaguide Complex, internal zone of the Betic Cordillera, southeast Spain. *Tectonics*, 12(2), 460–476. <https://doi.org/10.1029/92TC02507>
- Martín, J. M., Braga, J. C., & Rivas, P. (1989). Coral successions in Upper Tortonian reefs in SE Spain. *Lethaia*, 22(3), 271–286. <https://doi.org/10.1111/j.1502-3931.1989.tb01342.x>
- Martínez-Martos, M., Galindo-Zaldívar, J., Martínez-Moreno, F. J., Calvo-Rayó, R., & Sanz de Galdeano, C. (2017). Superposition of tectonic structures leading elongated intramontane basin: The Alhabia basin (Internal Zones, Betic Cordillera). *International Journal of Earth Sciences*, 106(7), 2461–2471. <https://doi.org/10.1007/s00531-016-1442-9>
- Martinius, A. W. (1991). Growth rates and population dynamics in *Crassostrea cf. rarilamella* from the Lower Eocene Roda Formation (southern Pyrenees, Spain). *Geologie en Mijnbouw*, 70(1), 59–73.
- Martín-Martín, J. M. (1996). *El Terciario del Dominio Malaguide en Sierra Espuña (Cordillera Bética oriental, SE España): Estratigrafía y evolución paleogeográfica*. Ph.D. Thesis, Universidad de Granada, 297 pp.
- Martín-Suárez, E., Freudenthal, M., & Agustí, J. (1993). Micromammals from the Middle Miocene of the Granada Basin (Spain). *Geobios*, 26(3), 377–387. [https://doi.org/10.1016/S0016-6995\(93\)80028-P](https://doi.org/10.1016/S0016-6995(93)80028-P)
- Miller, K. G., Browning, J. V., Schmelz, W. J., Kopp, R. E., Mountain, G. S., & Wright, J. D. (2020). Cenozoic sea-level and cryospheric evolution from deep-sea geochemical and continental margin records. *Science Advances*, 6(20), eaaz1346. <https://doi.org/10.1126/sciadv.aaz1346>
- Montenat, C. (Ed.). (1990). *Les bassins Néogènes du domaine bétique oriental (Espagne)* (p. 392). Documents et Travaux Institut Géologique Albert de Lapparent.
- Pascual-Molina, A. M. (1997). *La Cuenca Neógena de Tabernas (Cordilleras Béticas)*. Unpublished Ph.D. Thesis, Universidad de Granada, Spain, 345 pp.
- Perrin, C., & Bosellini, F. R. (2012). Paleobiogeography of scleractinian reef corals: Changing patterns during the Oligocene-Miocene climatic transition in the Mediterranean. *Earth Science Review*, 111(1–2), 1–24. <https://doi.org/10.1016/j.earscirev.2011.12.007>
- Perrin, C., & Bosellini, F. R. (2013). The Late Miocene coldspot of z-coral diversity in the Mediterranean: Patterns and causes. *Comptes Rendus Palevol*, 12(5), 245–255. <https://doi.org/10.1016/j.crpv.2013.05.010>
- Prager, E. J., & Ginsburg, R. N. (1989). Carbonate nodule growth on Florida's outer shelf and its implications for fossil interpretations. *Palaios*, 4(4), 310–317. <https://doi.org/10.2307/3514555>
- Rivas, P., Braga, J. C., & Sánchez-Almazo, I. M. (1999). Arrecifes del Tortonense inferior en la cuenca de Granada, Cordillera Bética, España. *Trabajos de Geología*, 21(21), 309–321. <https://doi.org/10.17811/tdg.21.1999.309-321>
- Rodríguez-Fernández, J. (1982). *El mioceno del sector central de las Cordilleras Béticas*. Ph.D. Thesis, Universidad de Granada, Spain, 224 pp.
- Rodríguez-Fernández, J., Sanz de Galdeano, C., & Serrano, F. (1990). Le couloir des Alpujarras. *Documents Et Travaux Institut Géologique Albert De Lapparent*, 12, 87–100.
- Rodríguez-López, J. P., & Arche, A. (2010). Deltas. In A. Arche (Ed.), *Sedimentología: Del proceso físico a la cuenca sedimentaria* (pp. 561–618). CSIC.
- Rondeel, H. E. (1965). *Geological investigations in the western Sierra Cabrera and adjoining areas*. Ph.D. Thesis, University of Amsterdam, The Netherlands, 161 pp.
- Rosen, B. R. (1999). Paleoclimatic implications of the energy hypothesis from Neogene corals of the Mediterranean region. In J. Agustí, L. Rook, & P. Andrews (Eds.), *The evolution of Neogene terrestrial ecosystems in Europe* (pp. 309–327). Cambridge University Press.

- Rustichelli, A., Agosta, F., Tondi, E., Galindo-Zaldívar, J., Di Celma, C., & Spina, V. (2013). Fault growth as a key control on the sedimentary architecture and depositional environments of extensional basins: The case study of the Tablate area (Granada Basin, Spain). *Italian Journal of Geosciences*, 132(3), 422–442. <https://doi.org/10.3301/IJG.2012.38>
- Santisteban, C., & Taberner, C. (1983). Shallow marine and continental conglomerates derived from coral reef complexes after desiccation of a deep marine basin: The Tortonian-Messinian deposits of the Fortuna Basin, SE Spain. *Journal of the Geological Society of London*, 140(3), 401–411. <https://doi.org/10.1144/gsjgs.140.3.0401>
- Sanz de Galdeano, C., & Alfaro, P. (2004). Tectonic significance of the present relief of the Betic Cordillera. *Geomorphology*, 63(3), 175–190. <https://doi.org/10.1016/j.geomorph.2004.04.002>
- Sanz de Galdeano, C., & López-Garrido, A. C. (2000). Las fallas tortonienas a cuaternarias entre Granada y la costa: El límite occidental del Nevado-Filábride y de las unidades alpujarrides inferiores. *Revista De La Sociedad Geológica De España*, 13(3–4), 519–528.
- Sanz de Galdeano, C., & Vera, J. A. (1992). Stratigraphic record and palaeogeographical context of the Neogene basins in the Betic Cordillera. *Spain. Basin Research*, 4(1), 21–36. <https://doi.org/10.1111/j.1365-2117.1992.tb00040.x>
- Sola, F., Braga, J. C., & Aguirre, J. (2013). Hooked and tubular coralline algae indicate seagrass beds associated to Mediterranean Messinian reefs (Poniente Basin, Almería, SE Spain). *Palaeogeography, Palaeoclimatology, Palaeoecology*, 374, 218–229. <https://doi.org/10.1016/j.palaeo.2013.01.020>
- Sola, F., Braga, J. C., & Sælen, G. (2022). Contradictory coeval vertical facies changes in Upper Miocene heterozoan carbonate–terrigenous deposits (Sierra de Gádor, Almería, SE Spain). *Journal of Sedimentary Research*, 92(3), 257–274. <https://doi.org/10.2110/jsr.2022.010>
- Soria, J. (1993). *La sedimentación neógena entre la Sierra Arana y el Río Guadiana Menor (Cordillera Bética Central)*. Ph.D. Thesis, Universidad de Granada, 292 pp.
- Soria, J. (1994). Sedimentación y tectónica durante el Mioceno en la región de Sierra Arana-Mencal y su relación con la evolución geodinámica de la Cordillera Bética. *Revista De La Sociedad Geológica De España*, 7(3–4), 199–213.
- Stenzel, H. B. (1971). Oysters. Treatise on Invertebrate Paleontology. In *Treatise on invertebrate paleontology*, Part N, Mollusca 6, 3, 953–1224.
- Vera, J. A. (1988). Evolución de los sistemas de depósito en el margen Ibérico de las Cordilleras Béticas. *Revista De La Sociedad Geológica De España*, 1(3–4), 373–391.
- Vermeij, M. J. A., Frade, P. R., Jacinto, R. I. R., Debrot, A. O., & Bak, R. P. M. (2007). Effects of reproductive mode on habitat-related differences in the population structure of eight Caribbean coral species. *Marine Ecology Progress Series*, 351, 91–102. <https://doi.org/10.3354/meps07085>
- Veron, J. E. N. (1995). *Corals in space and time: The biogeography and evolution of the Scleractinia*. Cornell University Press.
- Völk, H. R. (1967). *Zur geologie und stratigraphie des neogenenbeckens von Vera, Südost-Spanien*. Ph.D. Thesis, University of Amsterdam, 160 pp.
- Wade, B. S., Pearson, P. N., Berggren, W. A., & Pälike, H. (2011). Review and revision of Cenozoic tropical planktonic foraminiferal biostratigraphy and calibration to the geomagnetic polarity and astronomical time scale. *Earth-Science Reviews*, 104(1–3), 111–142. <https://doi.org/10.1016/j.earscirev.2010.09.003>
- Wood, R. (1993). Nutrients, predation and the history of reef-building. *Palaos*, 8(6), 526–543. <https://doi.org/10.2307/3515030>
- Young, J. R., Wade, B. S., & Huber, B. T. (2017). pforams@mikrotax website. <http://www.mikrotax.org/pforams> [accessed July 2022].